proteolysis contributes to various brain pathologies (Rosenberg et al. 1992; Nakagawa et al. 1994). The inhibition of MMP alters functional and structural correlates of differentiation-induced sprouting such as remodeling in the dentate gyrus of the hippocampus (Reeves et al. 2003). In a behavioral study, MMP-9 knock-out mice display impairments in long-term potentiation and hippocampal-dependent memory in a fear-conditioning memory task (Nagy et al. 2006).

Behavioral changes induced by METH are linked to its capacity to elevate extracellular dopamine levels through the redistribution of dopamine from synaptic vesicles to the cytosol and promotion of reverse transport (Sulzer et al. 1995; Nakajima et al. 2004). In the present study, the behavioral effects of TIMP-AS and doxycycline on the METH-induced behavioral sensitization were correlated to changes in the METH-induced increase in extracellular dopamine levels in the NAc: TIMP-AS potentiated while doxycycline reduced the METH-induced dopamine release. These findings are in agreement with our previous report that microinjection of purified human MMP-2 directly into the NAc significantly potentiated the acute METH-induced increase in extracellular dopamine levels in the NAc and that METH-induced dopamine release in the NAc was significantly decreased in the MMP-2-(−/−) and MMP-9-(−/−) mice compared with the response in wild-type mice (Mizoguchi et al. 2007).

The sensitivity of dopamine receptors to endogenous and exogenous ligands is known to be an important parameter of dopamine-related functions in physiology and pathology. Reduced signaling via Gi-coupled receptors may be an important neuroadaptation in cocaine addiction (Goldstein and Volkow 2002). G protein signaling in the Fc plays a crucial role as a potential pathological change contributing to cocaine sensitization and drug seeking (Bowers et al. 2004). Therefore we investigated the role of the MMP/TIMP system in repeated METH treatment-induced changes in dopamine D1 and D2 receptor signaling. TIMP-AS treatment exaggerated the repeated METH-induced impairment of dopamine D2 receptor agonist-stimulated [^{35}S]GTPγS binding without affecting the impairment of dopamine D1 receptor agonist-stimulated binding. In contrast, doxycycline ameliorated the impairment of D2 receptor agonist-stimulated [^{35}S]GTPγS binding. Although the effects of TIMP-AS and MMP inhibitors used in this study are not specific to MMP-2 and MMP-9, we also demonstrated that MMP-2-(−/−) and MMP-9-(−/−) mice showed some resistance to the inhibitory effect of repeated METH treatment on dopamine D2 agonist-stimulated [^{35}S]GTPγS binding. Therefore, these results suggest that the changes in the dopamine receptor signaling induced by repeated METH treatment is attributable to METH-induced expression of the MMP/TIMP system. Indeed, in vitro treatment of membranes with purified human MMP-2 reduced while TIMP-2 treatment enhanced dopamine D2 receptor agonist-stimulated [^{35}S]GTPγS binding although

they had no effect of the dopamine D1 receptor-stimulated binding. There were no differences in Gi protein levels between the TIMP-AS and TIMP-SC group, while METH treatment for 3 days decreased dopamine D2 receptor protein levels compared with the saline group (data not shown). Taken together, it is possible that the MMP-2 and MMP-9 are involved in the regulation of dopamine D2 receptor-mediated G protein signaling in the Fc. Because dopamine D2 receptors function as a feedback inhibition of dopamine release (Bowyer and Weiner 1987; Lindgren et al. 2001), their down-regulation may result in an enhancement of the METH-induced increase in extracelluar dopamine levels.

The molecular mechanisms by which the MMP/TIMP system regulates the METH-induced increase in extracelluar dopamine levels and the dopamine D2 receptor-mediated G protein signaling remain to be elucidated. It has been demonstrated that reverse activation of plasmalemmal dopamine transporter is involved in the METH-induced increase in extracellular dopamine levels. Degradation of ECM such as laminin by MMP may result in functional changes in plasmamembrane proteins such as dopamine transporter, dopamine receptors and G proteins. For instance, Freyer et al. (2004) have shown that ECM modulates Gi activity in human airway smooth muscle cells, and laminin in particular can activate Gi signaling. Laminin in the synaptic cleft localizes calcium channels to the sites of active zones (Sunderland et al. 2000) and induces a small but significant increase in calcium levels in ciliary ganglion neurons when applied in soluble form to the culture medium (Bixby et al. 1994). Alternatively, a recent study has indicated that cleavage of dystroglycan, which may be a target for MMP in the ECM, induces conformational changes that affect both pre- and postsynaptic elements (Kaczmarek et al. 2002). The deletion of neurexin, which is a pre-synaptic element for dystroglycan, in mice causes a severe reduction of Ca^{2+}-channel activity and a major decrease in evoked neurotransmitter release (Ushkaryov et al. 2002; Kattenstroth et al. 2004). Neurexin can also regulate the post-synaptic N-methyl-D-asparatate receptor function (Kattenstroth et al. 2004).

In conclusion, our findings suggest that the MMP-2, MMP-9 and TIMP-2 are involved in the rearrangement of the neural network in the mesocorticolimbic dopamine system, which plays a role in the development of behavioral sensitization to METH. It is speculated that the activation of the MMP/TIMP system in the Fc evoked by repeated METH treatment induces the cleavage of ECM such as laminin, resulting in an increase in the METH-induced dopamine release as well as a reduction in the efficacy of dopamine D2 receptor-mediated G protein signaling.

Acknowledgements

References

Asahi M., Wang X., Mori T., Sumii T., Jung J. C., Moskowitz M. A., Fini M. E. and Lo E. H. (2001) Effects of matrix metalloproteinases-9 gene knock-out on the proteolysis of blood-brain barrier and white matter components after cerebral ischemia. *J. Neurosci.* 21, 7724–7732.

Berke J. and Hyman S. T. (2000) Addiction, dopamine, and the molecular mechanisms of memory. *Neuron* 25, 515–532.

Beyer C. E. and Steketee J. (2002) Cocaine sensitization: modulation by dopamine D2 receptors. *Cereb. Cortex* 12, 526–535.

Bilousova T. V., Rusakov D. A., Ethell D. W. and Ethell I. M. (2006) Matrix metalloproteinase-7 disrupts dendritic spines in hippocampal neurons through NMDA receptor activation. *J. Neurochem.* 97, 44–56.

Bixby J. L., Grunwald G. B. and Bookman R. J. (1994) Ca^{2+} influx and neurite growth in response to purified N-cadherin and laminin. *J. Cell Biol.* 127, 1461–1475.

Bowers M. S., McFarland K., Lake R. W., Peterson Y. K., Lapish C. C., Gregory M. L., Lanier S. M. and Kalivas P. W. (2004) Activator of G protein signaling 3: a gatekeeper of cocaine sensitization and drug seeking. *Neuron* 42, 269–281.

Bowyer J. F. and Weiner N. (1987) Modulation of the Ca^{2+}-evoked release of [3H]-dopamine from striatal synaptosomes by dopamine (D2) agonists and antagonists. *J. Pharmacol. Exp. Ther.* 241, 27–33.

Frankin K. B. J. and Paxinos G. (1997) *The mouse brain in stereotaxic coordinates.* Academic, San Diego.

Freyer A. M., Bilington C. K., Penn R. B. and Hall I. P. (2004) Extracellular matrix modulates β2-adrenergic receptor signaling in human airway smooth muscle cells. *Am. J. Respir. Cell Mol. Biol.* 31, 440–445.

Goldstein R. Z. and Volkow N. D. (2002) Drug addiction and its underlying neurobiological basis: neuroimaging evidence for the involvement of the frontal cortex. *Am. J. Psychiatry* 159, 1642–1652.

Hashimoto T., Matsumoto M. M., Li J. F., Lawton M. T. and Young W. L. (2005) Suppression of MMP-9 by doxycycline in brain arteriovenous malformations. *BMC Neurology* 5, 1.

Itoh T., Ikeda T., Gomi H., Nakao S., Suzuki T. and Itohara S. (1997) Unaltered secretion of β-amyloid precursor protein in gelatinase A (matrix metalloproteinases 2)-deficient mice. *J. Biol Chem.* 272, 22389–22392.

Kaczmarek L., Lapinska-Dzwonek J. and Szymczak S. (2002) Matrix metalloproteinases in the adult brain physiology: a link between c-Fos, AP-1 and remodeling of neuronal connections? *EMBO J.* 21, 6643–6648.

Kattenstroth G., Tantalaki E., Sudhof T. C., Gottmann K. and Missler M. (2004) Postsynaptic N-methyl-D-aspartate receptor function requires α-neurexins. *Proc. Natl Acad. Sci. USA* 101, 2607–2612.

Khokha R., Waterhouse P., Yagel S., Lala P. K., Overall C. M., Norton G. and Denhardt D. T. (1989) Antisense RNA-induced reduction in murine TIMP levels confers oncogenicity on Swiss 3T3 cells. *Science* 243, 947–950.

Koivunen E., Arap W., Valtanen H. *et al.* (1999) Tumor targeting with a selective gelatinase inhibitor. *Nat. Biotechnol.* 17, 768–774.

Lee S. R., Tsuji K., Lee S. R. and Lo E. H. (2004) Role of matrix metalloproteinases in delayed neuronal damage after transient global cerebral ischemia. *J. Neurosci.* 24, 671–678.

Lindgren N., Xu Z.-Q., Herrera-M M., Haycock J., Hokfelt T. and Fisone G. (2001) Dopamine D2 receptors regulate tyrosine hydroxylase activity and phosphorylation at Ser40 in rat striatum. *Eur. J. Neurosci.* 13, 773–780.

Mannello F. and Gazzanelli G. (2001) Tissue inhibitors of metalloproteinases and programmed cell death: conundrums, controversies and potential implications. *Apoptosis* 6, 479–482.

Mizoguchi H., Yamada K., Mizuno M., Mizuno T., Nitta A., Noda Y. and Nabeshima T. (2004) Regulations of methamphetamine reward by extracellular signal-regulated kinase 1/2/ets-like gene-1 signaling pathway via the activation of dopamine receptors. *Mol. Pharmacol.* 65, 1293–1301.

Mizoguchi H., Yamada K., Niwa M., Mouri A., Mizuno T., Noda Y., Nitta A., Itohara S., Banno Y. and Nabeshima T. (2007) Reduction of methamphetamine-induced sensitization and reward in matrix metalloproteinase-2 and -9 deficient mice. *J. Neurochem.* 100, 1579–1588.

Nagai T., Yamada K., Yoshimura M., Ishikawa K., Miyamoto Y., Hashimoto K., Noda Y., Nitta A. and Nabeshima T. (2004) The tissue plasminogen activator-plasmin system participates in the rewarding effect of morphine by regulating dopamine release. *Proc. Natl Acad. Sci. USA* 101, 3650–3655.

Nagai T., Noda Y., Ishikawa K., Miyamoto Y., Yoshimura M., Ito M., Takayanagi M., Takuma K., Yamada K. and Nabeshima T. (2005) The role of tissue plasminogen activator in methamphetamine-related reward and sensitization. *J. Neurochem.* 92, 660–667.

Nagy V., Bozdagi O., Matynia A., Balcerzyk M., Okulski P., Dzwonek J., Costa R. M., Silva A. J., Kaczmarek L. and Huntley G. W. (2006) Matrix metalloproteinase-9 is required for hippocampal late-phase long-term potentiation and memory. *J. Neurosci.* 15, 1923–1934.

Nakagawa T., Kubota T., Kabut M., Sato K., Kawano H., Hayakawa T. and Okada Y. (1994) Production of matrix metalloproteinases and tissue inhibitor of metalloproteinases-1 by human brain tumors. *J. Neurosurg.* 81, 69–77.

Nakajima A., Yamada K., Nagai T. *et al.* (2004) Role of tumor necrosis factor-alpha in methamphetamine-induced drug dependence and neurotoxicity. *J. Neurosci.* 24, 2212–2225.

Nestler E. J. (2001) Molecular basis of long-term plasticity underlying addiction. *Nat. Rev. Neurosci.* 2, 119–128.

Paxinos G. and Watson C. (1982) *The Rat Brain in Stereotaxic Coordinates.* Academic, New York.

Reeves T., Prins M. L., Zhu J. P., Povlishock J. T. and Phillips L. L. (2003) Matrix metalloproteinases inhibition alters functional and structural correlates of deafferentation-induced sprouting in the dentate gyrus. *J. Neurosci.* 12, 10182–10189.

Rivera S., Tremblay E., Timsit S., Canals O., Ben-Ari Y. and Khrestchatisky M. (1997) Tissue inhibitor of metalloproteinases-1 (TIMP-1) is differentially induced in neurons and astrocytes after seizures: evidence for developmental, immediate early gene, and lesion response. *J. Neurosci.* 17, 4223–4235.

Robinson T. E. and Kolb B. (1997) Persistent structural modifications in nucleus accumbens and prefrontal cortex neurons produced by previous experience with amphetamine. *J. Neurosci.* 17, 8491–8497.

Rosenberg G. A., Kornfeld M., Estrada E., Kelly R. O., Liotta L. A. and Stetler-Stevenson W. G. (1992) TIMP-2 reduces proteolytic opening of blood-brain barrier by IV collagenagse. *Brain Res.* 56, 203–207.

Shippenberg T. S. and Heidbreder C. h. (1995) Sensitization to the conditioned rewarding effects of cocaine: pharmacological and temporal characteristics. *J. Pharmacol. Exp. Ther.* 273, 808–815.

Smith G. N. J., Brandt K. D. and Hasty K. A. (1996) Activation of recombinant human neutrophil procollagenase in the presence of doxycycline results in fragmentation of the enzyme and loss of enzyme activity. *Arthritis Rheum.* **39**, 235–244.

Sternlicht M. D. and Werb Z. (2001) How matrix metalloproteinases regulate cell behavior. *Annu. Rev. Cell Dev. Biol.* **17**, 463–516.

Strongin A. Y., Collier I., Bannikov G., Marmer B. L., Grant G. A. and Goldberg G. I. (1995) Mechanism of cell surgace activation of 72-kDa type IV collagenase Isolation of the activated form of the membrane metalloproteinases. . *J. Biol. Chem.* **270**, 5331–5338.

Sulzer D., Chen T. K., Lau Y. Y., Kristensen H., Rayport S. and Ewing A. (1995) Amphetamine redistributes dopamine from synaptic vesicles to the cytosol and promotes reverse transport. *J. Neurosci.* **15**, 4102–4108.

Sunderland W. J., Son Y. J., Miner J. H., Sanes J. R. and Carlson S. S. (2000) The presynaptic calcium channel is part of a transmembrane complex linking a synaptic laminin ($\alpha4\beta2\gamma1$) with non-erythroid spectrin. *J. Neurosci.* **20**, 1009–1019.

Szklarczyk A., Lapinska J., Rylski M., Mckay R. D. and Kaczmarek L. (2002) Matrixmetalloproteinase-9 undergoes expression and activation during dendritic remodeling in adult hippocampus. *J. Neurosci.* **22**, 920–930.

Uitto V. J., Firth J., Nip L. and Golub L. (1994) Doxycycline and chemically modified tetracyclines inhibit gelatinase A (MMP-2) gene expression in human skin keratinocytes. *Ann. NY Acad. Sci.* **732**, 140–151.

Ushkaryov Y. A., Petrenko A. G., Geppert M. and Sudhof T. C. (2002) Neurexins: synaptic cell surface proteins related to the alpha-latrotoxin receptor and laminin. *Science* **257**, 50–56.

Vaillant C., Didier-Bazes M., Hurter A., Bein M. F. and Thomasset N. (1999) Spatiotemporal expression patterns of metalloproteinases and their inhibitors in the postnatal developing rat cerebellum. *J. Neurosci.* **19**, 4994–5004.

Wright J. W., Reichert J. R., Davis C. J. and Harding J. W. (2002) Neural plasticity and the brain renin-angiotensin system. *Neurosci. Biovehav. Rev.* **26**, 529–552.

Yamada K., Nagai T. and Nabeshima T. (2005) Drug dependence, synaptic plasticity, and tissue plasminogen activator. *J. Pharmacol. Sci.* **97**, 157–161.

Yong V. W., Power C., Forsyth P. and Edwards D. R. (2001) Metalloproteinases in biology and pathology of the nervous system. *Nat. Rev. Neurosci.* **2**, 502–511.

Zhang J. W. and Gottschall P. E. (1997) Zymographic measurement of gelatinase activiy in brain tissue after detergent extrqaction and affinity-support purification. *J. Neurosci. Methods* **76**, 15–20.

Behavioral/Systems/Cognitive

A Novel Molecule "Shati" Is Involved in Methamphetamine-Induced Hyperlocomotion, Sensitization, and Conditioned Place Preference

Minae Niwa,[1,3] Atsumi Nitta,[1] Hiroyuki Mizoguchi,[1] Yasutomo Ito,[2] Yukihiro Noda,[1] Taku Nagai,[1] and Toshitaka Nabeshima[1,3]

[1]Department of Neuropsychopharmacology and Hospital Pharmacy and [2]Equipment Center for Research and Education, Nagoya University Graduate School of Medicine, Nagoya 466-8560, Japan, and [3]Department of Chemical Pharmacology, Meijo University Graduate School of Pharmaceutical Sciences, Nagoya 468-8503, Japan

Drug addiction places an enormous burden on society through its repercussions on crime rate and healthcare. Repeated exposure to drugs of abuse causes cellular adaptations in specific neuronal populations that ultimately can lead to a state of addiction. In the present study, we have identified a novel molecule "shati" from the nucleus accumbens (NAc) of mice treated with methamphetamine (METH) using the PCR-select complementary DNA subtraction method. Moreover, we investigated whether shati is involved in METH-induced hyperlocomotion, sensitization, and conditioned place preference (CPP). METH induced expression of shati mRNA dose dependently via dopamine (DA) receptors. We prepared antibodies against shati and, using them, found shati to be expressed in neuronal cells of the mouse brain. Treatment with the shati antisense oligonucleotide (shati-AS), which significantly inhibited the expression of shati mRNA, enhanced the acute METH response, METH-induced behavioral sensitization, and CPP. Blockage of shati mRNA by shati-AS potentiated the METH-induced increase of DA overflow in the NAc and the METH-induced decrease in synaptosomal and vesicular DA uptake in the midbrain. These results suggest that a novel molecule shati is involved in the development of METH-induced hyperlocomotion, sensitization, and CPP. The functional roles of shati in METH-regulated behavioral alternations are likely to be mediated by its inhibitory effects on the METH-induced increase of DA overflow in the NAc and the METH-induced decrease in DA uptake in the midbrain.

Key words: shati; methamphetamine; behavioral sensitization; conditioned place preference; dopamine; addiction

Introduction

In terms of lost lives and productivity, drug dependence remains one of the most serious threats to the public health of a nation (Nestler, 2002). Drugs of abuse, including methamphetamine (METH), modulate the activity of mesolimbic dopaminergic

neurons, projecting from the ventral tegmental area (VTA) to the nucleus accumbens (NAc) (Koob, 1992; Wise, 1996b; Koob et al., 1998). The psychostimulatory effects of METH are associated with an increase in extracellular dopamine (DA) levels in the brain, by facilitating the release of DA from presynaptic nerve terminals and inhibiting reuptake (Heikkila et al., 1975; Seiden et al., 1993; Giros et al., 1996). In rodent, augmentation of behavioral responses to psychostimulants is observed during and after their repeated administration. Therefore, it has been proposed that activity-dependent synaptic plasticity and remodeling of the mesolimbic dopaminergic system may play a crucial role in drug dependence (Nestler, 2001; Yamada and Nabeshima, 2004).

Using cDNA microarrays, changes in the mRNA expression profile in relevant brain regions (e.g., NAc) have been assessed after chronic administration of abused drugs (Douglass and Daoud, 1996; Cha et al., 1997; Wang et al., 1997). Evidence from this line of research has implicated nuclear factor-κB (Ang et al., 2001) and ΔFosB (Zachariou et al., 2006) in signal transduction pathways that modulate behavioral effects induced by drugs and contribute to long-term neuronal changes associated with dependence (Laakso et al., 2002). To elucidate the mechanism, caused by chronic drug abuse, of stable changes in the brain that play a role in the long-lasting behavioral abnormalities of dependent subjects, the candidates for drug-dependence-related genes

whose expression was altered by repeated administration of METH or morphine (MOR) were screened by using cDNA microarray. Recently, there are many studies that showed that cytokines/neurotrophic factors and extracellular matrix/proteases play critical roles in activity-dependent synaptic plasticity and remodeling of the mesocorticolimbic dopaminergic system (Horger et al., 1999; Messer et al., 2000; Mizoguchi et al., 2007). We found that tumor necrosis factor-α (TNF-α) plays a neuroprotective role in METH-induced dependence and neurotoxicity (Nakajima et al., 2004) and reduces MOR-induced rewarding effects and behavioral sensitization (Niwa et al., 2007a,d). Furthermore, the rewarding effects and sensitization induced by METH and MOR are attenuated by Leu-Ile, an inducer of TNF-α, and glial cell line-derived neurotrophic factor (GDNF) (Niwa et al., 2007a-d). The tissue plasminogen activator (tPA)–plasmin system potentiates the rewarding and locomotor-stimulating effects of METH, MOR, and nicotine by regulating release of DA (Nagai et al., 2004, 2005a,b, 2006). However, the exact neuronal circuits and molecular cascade essential for drug dependence remain unclear. Therefore, we attempt to explore the novel molecules that play more critical roles in drug dependence, because the functions of molecules targeted by DNA microarray screening have been already well known.

In the present study, we identified a novel molecule "shati" from the NAc of mice treated with METH using the PCR-select cDNA subtraction method, which is a differential and epochal cloning technique. Moreover, we demonstrated that shati is involved in the METH-induced hyperlocomotion, sensitization, and conditioned place preference (CPP).

Materials and Methods

Animals. The male C57BL/6J inbred mice were obtained from SLC Japan (Hamamatsu, Japan). Animals were housed in plastic cages and kept in a temperature-, humidity-, and light-controlled room (23 ± 1°C; 50 ± 5% humidity; 12 h light/dark cycle starting at 8:00 A.M.) and had *ad libitum* access to food and water, except during behavioral experiments. All animal care and use was in accordance with the National Institutes of Health *Guide for the Care and Use of Laboratory Animals* and approved by the Institutional Animal Care and Use Committee of Nagoya University School of Medicine. Animals were treated according to the *Guidelines of Experimental Animal Care* issued from the Office of the Prime Minister of Japan.

PCR-select cDNA subtraction. Mice were administered METH (2 mg/kg, s.c.) or saline for 6 d and took NAc 2 h after the last injection of METH. PCR-select cDNA subtraction (Clontech, Palo Alto, CA) was performed using a previously established procedure (Diatchenko et al., 1996; Gurskaya et al., 1996) to detect the genes in the NAc affected by METH treatment. Briefly, they involve hybridization of cDNA from one population (tester; METH-treated NAc) to excess of mRNA (cDNA) from other population (driver; saline-treated NAc) and then separation of the unhybridized fraction (target) from hybridized common sequences. Total RNAs were extracted by RNeasy Max (Qiagen, Hilden, Germany). For each subtraction, we performed two PCR amplifications. Products from the secondary PCRs were inserted into pCRII using a T/A cloning kit (Invitrogen, Carlsbad, CA). Plasmid or cosmid DNAs were prepared using QIAwell 8 Plus kit (Qiagen) according to the protocol of the manufacturer. Nucleic acid homology searches were performed using the BLAST (basic local alignment search tool) program through e-mail servers at the National Center for Biotechnology Information (NCBI) (National Institutes of Health, Bethesda, MD).

Structure models. Homology modeling for C-terminal domain of shati was established using Molecular Operating Environment (MOE) software (Chemical Computing Group, Montreal, Quebec, Canada). Molecular mechanics calculations were performed by using an MMFF94x force field. Docking simulations of acetyl-CoA or ATP with shati protein were

Table 1. Primers sequences and their targets for RT-PCR

Primer	Sequence	Target (bp)
1		
Forward	5'-CTTGCCTCCCCAGCCCATCA-3'	1987–2006
Reverse	5'-CTGGGGGCCAGGGTTCTGCT-3'	2147–2166
2		
Forward	5'-GGGTGGCCGGGTAGGTGGAA-3'	2909–2928
Reverse	5'-GGCAGTGCCCAGCCCTTCCT-3'	3073–3092
3		
Forward	5'-TGTACATTCCTCCCTGGTGGTG-3'	3521–3542
Reverse	5'-AAATCTGAGAGCTGCAAGAAAATAGGG-3'	3594–3620

The amplification consisted of an initial step (95°C for 5 min) and then 35 cycles of denaturation for 30 s at 94°C and annealing for 1 min at 70, 71, and 65°C.

also examined using MOE software (Chemical Computing Group) to calculate the interactive potential energy of molecules.

Reverse transcription-PCR and real-time reverse transcription-PCR. Mice were administered METH (0.3, 1, and 2 mg/kg, s.c., once a day for 3 or 6 d) and decapitated 2 h after the last injection of METH. In the real-time reverse transcription (RT)-PCR experiment on the antagonism of METH-induced shati mRNA expression, mice were treated with the DA D$_1$-like receptor antagonist R(+)-SCH23390 [R(+)-7-chloro-8-hydroxy-3-methyl-1-phenyl-2,3,4,5-tetrahydro-1H-3-benzazepine] (0.1 mg/kg, i.p.) or DA D$_2$-like receptor antagonist raclopride (2 mg/kg, i.p.) 30 min before METH (2 mg/kg, s.c.) once a day for 6 d. Functionally, R(+)-SCH23390 (0.1–0.5 mg/kg) is a potent blocker of stereotyped behaviors and increased locomotion induced by amphetamine or apomorphine (Christensen et al., 1984; Napier et al., 1986). The increase in TNF-α or tPA mRNA expression in the NAc induced by METH is inhibited by pretreatment with either R(+)-SCH23390 (0.1 or 0.5 mg/kg, i.p.) or raclopride (2 mg/kg, i.p.) (Nakajima et al., 2004; Nagai et al., 2005a). R(+)-SCH23390 at the dose of 0.1 mg/kg, not 0.03 mg/kg, significantly inhibits the hyperphosphorylation of extracellular signal-regulated kinase 1/2 in the NAc and striatum evoked by METH-induced CPP as well as the expression of CPP in METH-treated animals (Mizoguchi et al., 2004). Depending on these evidences, we selected the doses of R(+)-SCH23390 at 0.1 mg/kg and raclopride at 2 mg/kg.

Total RNA was isolated using an RNeasy kit (Qiagen) and converted into cDNA using a SuperScript First-Strand System for RT-PCR kit (Invitrogen). The primers used for RT-PCR were as follows: 5'-CTTGCCTCCCCAGCCCATCA-3' (forward-1; base pairs 1987–2006) and 5'-CTGGGGGCCAGGGTTCTGCT-3' (reverse-1; base pairs 2147–2166) for set of sequences 1; 5'-GGGTGGCCGGGTAGGTGGAA-3' (forward-2; base pairs 2909–2928) and 5'-GGCAGTGCCCAGC-CCTTCCT-3' (reverse-2; base pairs 3073–3092) for set of sequences 2; and 5'-TGTACATTCCTCCCTGGTGGTG-3' (forward-3; base pairs 3521–3542) and 5'-AAATCTGAGAGCTGCAAGAAAATAGGG-3' (reverse-3; base pairs 3594–3620) for set of sequences 3 (Table 1). The amplification consisted of an initial step (95°C for 5 min) and then 35 cycles of denaturation for 30 s at 94°C and annealing for 1 min at 70, 71, and 65°C in a GeneAmp PCR System 9700 (Applied Biosystems, Foster City, CA). The levels of shati and TNF-α mRNA were determined by real-time RT-PCR using a TaqMan probe. The 18S ribosomal RNA was used as the internal control (PE Applied Biosystems, Foster City, CA). The mouse shati primers used for real-time RT-PCR were as follows: 5'-TGTAAACACCCCTAAAGTGCCCT-3' (forward; base pairs 2967–2989) and 5'-TCAATCCTGCATACAAGGAATCAA-3' (reverse; base pairs 3022–3045); and TaqMan probe, 5'-CACAGTCTGTGAGG-CTCAGGTTGCCC-3' (probe; base pairs 2995–3020). The amplification consisted of an initial step (95°C for 5 min) and then 40 cycles of denaturation for 30 s at 95°C and annealing for 1 min at 59°C in an iCycle iQ Detection System (Bio-Rad, Hercules, CA). The expression levels were calculated as described previously (Wada et al., 2000).

Immunohistochemistry. Two antibodies against the peptide of the hypothetical protein, CNTAFRGLRQHPRTQLL (S-3) and CMSVDSR-FRGKGIAKALG (S-4), unique to shati were generated. These peptides were conjugated to the keyhole limpet hemocyanin and injected into rabbits six times at 1 week intervals. Serum was taken from the rabbits 1

week after the final injection of these peptides. The serum was diluted 200 times used for the immunostaining.

For immunohistochemical analysis, mice were killed 24 h after repeated treatment with METH (2 mg/kg, s.c., once a day for 6 d). The brains were sliced at 20 μm in the cryostat. Polyclonal rabbit anti-S-3 or S-4 antibody (1:200), monoclonal mouse anti-neuron-specific nuclear antigen (NeuN) antibody (1:200; Chemicon, Temecula, CA), and monoclonal mouse anti-glial fibrillary acidic protein (GFAP) antibody (1:200; Chemicon) served as primary antibodies. Goat anti-mouse Alexa Fluor 546 (1:1000; Invitrogen) and goat anti-rabbit Alexa Fluor 488 (1:1000; Invitrogen) were used as secondary antibodies. Each stained slice was observed under a fluorescence microscope (Axioskoop 2 plus; Zeiss, Jena, Germany) and checked with Axiovision 3.0 systems (Zeiss).

Shati-antisense oligonucleotide treatment. Mice were anesthetized with pentobarbital (40 mg/kg, i.p.) and placed in a stereotaxic apparatus. The infusion cannula was connected to a miniosmotic pump (total capacity was 90 μl, Alzet 1002; Alza, Palo Alto, CA) filled with shati-antisense oligonucleotide (shati-AS) and -scramble oligonucleotide (shati-SC) and was implanted into the right ventricle [anteroposterior (AP) −0.5 mm, mediolateral (ML) +1.0 mm from the bregma, and dorsoventral (DV) −2.0 mm from the skull, according to the atlas of Franklin and Paxinos (1997)]. No histological or mechanical disruption was produced by implantation of the infusion cannula (data not shown). Phosphorothionate oligonucleotides were custom synthesized at Nisshinbo Biotechnology (Tokyo, Japan) and dissolved in artificial CSF (in mM: 147 NaCl, 3 KCl, 1.2 CaCl$_2$, and 1.0 MgCl$_2$, pH 7.2). We used shati-SC as a control of shati-AS, because we should deny the secondary effects on other genes or toxic effects, and we selected the design of shati-AS, which does not affect the other genes and already have been identified. The oligonucleotides were phosphorothionated at the three bases of both 5′ and 3′ ends, which results in increased stability and less toxicity. The sequences of shati-AS and shati-SC were 5′-TCTTCGTCTCGCAGACCATGTCG-3′ and 5′-GGTCTGCTACACTGCTGCTAGTC-3′, respectively. Shati-AS and shati-SC were continuously infused into the cerebral ventricle at a dose of 1.8 nmol/6 μl per day (flow rate, 0.25 μl/h). Additionally, shati-SC was used as a control. Three days after the start of oligonucleotide infusion, mice were subjected to METH treatment for sensitization.

Locomotor activity. Locomotor activity was measured using an infrared detector (Neuroscience Company, Tokyo, Japan) in a plastic box (32 × 22 × 15 cm high) and determined as described previously (Nakajima et al., 2004; Niwa et al., 2007b,d). One day after the start of oligonucleotide infusion, mice were habituated for 3 h in the box for 2 d and then administered METH (1 mg/kg, s.c.) or saline once a day for 5 d. Locomotor activity was measured for 2 h immediately after the METH or saline administration.

In vivo microdialysis. Mice were anesthetized with sodium pentobarbital, and a guide cannula (AG-8; EICOM, Kyoto, Japan) was implanted into the NAc (AP +1.7 mm, ML +0.8 mm mediolateral from the bregma, and DV −4.0 mm from the skull) according to the atlas of Franklin and Paxinos (1997) and secured to the skull using stainless steel screws and dental acrylic cement. Mice were administered METH (1 mg/kg, s.c.) 3 d after implantation of the guide cannula and the start of oligonucleotide infusion. One day after METH treatment for 2 d, a dialysis probe (AI-8-1, 1 mm membrane length; EICOM) was inserted through the guide cannula and perfused continuously with CSF (in mM: 147 NaCl, 4 KCl, and 2.3 CaCl$_2$) at a flow rate of 1.0 μl/min. Dialysate was collected in 20 min fractions and injected into the HPLC system (EICOM) for the measurement of DA levels. Three samples were used to establish baseline levels of DA before the administration of METH (1 mg/kg, s.c.).

Synaptosomal [³H]DA uptake. Three days after the start of oligonucleotide infusion, mice were subjected to METH treatment once a day for 3 d. Mice were decapitated 1 h after the final METH treatment. Midbrain synaptosomal [³H]DA uptake was determined as described previously (Fleckenstein et al., 1997; Nakajima et al., 2004; Niwa et al., 2007b). The final concentration of [³H]DA (PerkinElmer, Wellesley, MA) was 5 nM. Samples were incubated at 37°C for 4 min, and then ice-cold Krebs–Ringer's solution containing 10 μM GBR12909 [1-(2[bis(4-fluorophenyl-)methoxy]ethyl)-4-(3-phenylpropyl)piperazine] bimesy-

late hydrate] (Sigma, St. Louis, MO), a specific DA uptake inhibitor, was added. Nonspecific values were determined in the presence of 100 μM GBR12909 during the incubation. The radioactivity trapped on filters was measured with a liquid scintillation counter (Beckman Coulter, Fullerton, CA).

Vesicular [³H]DA uptake. Vesicular [³H]DA uptake was determined as described by Erickson et al. (1990). Synaptosomes were prepared as described by Nakajima et al. (2004). Vesicular [³H]DA uptake was performed by incubating synaptic vesicle samples (15 μg protein/100 μl) at 30°C for 4 min in assay buffer (in mM: 25 HEPES, 100 potassium tartrate, 1.7 ascorbic acid, 0.05 EGTA, 0.1 EDTA, and 2 ATP-Mg^{2+}, pH 7.0) in the presence of 30 nM [³H]DA (PerkinElmer). The reaction was terminated by the addition of 1 ml of cold wash buffer (assay buffer containing 2 mM MgSO$_4$ substituted for the ATP-Mg^{2+}, pH 7.0) and rapid filtration. Nonspecific values were determined by measuring vesicular [³H]DA uptake at 4°C. The radioactivity was measured with a liquid scintillation counter (Beckman Coulter).

Conditioned place preference. The apparatus used for the place conditioning task consisted of two compartments: a transparent Plexiglas box and a black Plexiglas box (both 15 × 15 × 15 cm high). To enable mice to distinguish easily the two compartments, the floors of the transparent and black boxes were covered with white plastic mesh and black frosting Plexiglas, respectively. Each box could be divided by a sliding door (10 × 15 cm high). The place conditioning paradigm was performed by using a previously established procedure with a minor modification (Noda et al., 1998; Schechter and Calcagnetti, 1998; Niwa et al., 2007a,b,d). In the preconditioning test, the sliding door was opened, and the mouse was allowed to move freely between both boxes for 15 min once a day for 3 d. On the third day of the preconditioning test, we measured the time that the mouse spent in the black and transparent boxes by using a Scanet SV-20 LD (Melquest, Toyama, Japan). The box in which the mouse spent the most time was referred to as the "preferred side" and the other box as the "nonpreferred side." Conditioning was performed during 6 successive days. Mice were given METH or saline in the apparatus with the sliding door closed. That is, a mouse was subcutaneously given METH and put in its nonpreferred side for 20 min. On the next day, the mouse was given saline and placed opposite the drug conditioning site for 20 min. These treatments were repeated for three cycles (6 d). In the postconditioning test, the sliding door was opened, and we measured the time that the mouse spent in the black and transparent boxes for 15 min, using the Scanet SV-20 LD. Place conditioning behavior was expressed by Post-Pre, which was calculated as: [(postvalue) − (prevalue)], where postvalue and prevalue were the difference in time spent at the drug conditioning and the saline conditioning sites in the postconditioning and preconditioning tests, respectively.

Statistical analysis. All data were expressed as means ± SE. Statistical differences between two groups were determined with Student's t test. Statistical differences among more than three groups were determined using a one-way ANOVA, two-way ANOVA, or an ANOVA with repeated measures (two or three-factor), followed by the Bonferroni's multiple comparison test (Bonferroni's correction; 3, 6, 15, and 36 comparisons in 3, 4, 6, and 9 groups, respectively). $p < 0.05$ was regarded as statistically significant.

Nucleotide sequences. The DNA Data Bank of Japan/GenBank/European Molecular Biology Laboratory accession number for the primary nucleotide sequence of shati is DQ174094.

Results

Identification of shati

The reasons why we pursued shati for intensive investigation arose from our preliminary findings with the PCR-select cDNA subtraction method to detect the genes in the NAc affected by METH treatment: mice were administrated METH (2 mg/kg, s.c.) or saline for 6 d, and shati mRNA production in the NAc was found to increase by 640% in METH-treated mice with robust behavioral sensitization compared with saline-treated mice (data not shown). The sequence of cDNA was completely matched to accession number NM_001001985 of NCBI gene bank (the gene

record was replaced by accession number NM_001001985.2 on April, 10, 2005). The sequence has been identified by the Mammalian Gene Collection Program Team (Strausberg et al., 2002). Blackshaw et al. (2004) has demonstrated the extended cDNA sequence by serial analysis of gene expression methods, which provides an unbiased and nearly comprehensive readout of gene expression and that the gene was for one of the proteins related to the retina development. We named this novel molecule shati after the symbol at Nagoya castle in Japan. The sequence is translated to a protein LOC269642 (accession number is NP_001001985.1 and 2; 001001985.1 was a part of 001001985.2) (supplemental Fig. 1, available at www.jneurosci.org as supplemental material).

Characterization of shati

Homology modeling for C-terminal domain of shati was established using MOE software (Chemical Computing Group) (Fig. 1A,B). Red character in Figure 1A showed homology modeling of shati. From motif analysis of shati, shati contained the sequence of GCN5-related N-acetyltransferase (GCAT) (Fig. 1C). Underlined character in Figure 1A showed GNAT motif. Docking simulations of acetyl-CoA or ATP with shati protein were also examined using MOE software (Chemical Computing Group) to calculate the interactive potential energy of molecules. Shati also contained acetyl-CoA binding or ATP binding site, because the analysis showed the lowest interactive potential energy of shati with acetyl-CoA or ATP, −301 and −322 kcal, respectively (supplemental Fig. 2, available at www.jneurosci.org as supplemental material). Docking simulations of shati with DA, DNA binding site, and nuclear localization signals showed too high interactive potential energy of molecules or no domain.

Expression of shati mRNA

As shown in Figure 2A, RT-PCR analysis revealed that shati is expressed at high levels in the cerebrum, cerebellum, liver, kidney, and spleen. We amplified and analyzed its three different target sequences by RT-PCR (Table 1). Similar results of RT-PCR were obtained with three different sets of primers (Fig. 2A).

We performed a series of experiments to validate the results of cDNA subtraction. Repeated METH treatment (2 mg/kg, s.c.) for 6 d significantly elevated the mRNA levels of the target sequences of shati in the NAc (Fig. 2B).

METH-induced expression of shati mRNA in the brain

As an initial step in assessing the relationship between shati and METH-induced sensitization and dependence, we examined whether single and repeated METH treatment altered the expression of shati mRNA in the mouse brain using the real-time RT-PCR method. The effects of repeated METH treatment (0.3, 1 and 2 mg/kg, s.c. for 3 d) on shati mRNA expression in the NAc were dose dependent ($F_{(3,28)}$ = 5.503; $p < 0.01$, one-way ANOVA) (Fig. 3A). The levels of shati mRNA were significantly increased 2, 6, and 24 h after the last METH treatment and then returned to control value 1 week after the treatment ($F_{(6,41)}$ = 4.444; $p < 0.01$, one-way ANOVA) (Fig. 3B). Single METH treatment (2 mg/kg, s.c.) remarkably induced shati mRNA expression in the NAc and hippocampus (Hip). METH (2 mg/kg, s.c.) or saline challenge on day 6 after repeated administration of METH (2 mg/kg, s.c.) for 5 d remarkably induced shati mRNA expression in the frontal cortex (Fc), NAc, and caudate-putamen (CPu) (repeated drug administration, $F_{(1,32)}$ = 20.368, $p < 0.01$ for Fc; single administration, $F_{(1,32)}$ = 0.005, $p = 0.942$ for Fc; repeated drug administration × single administration, $F_{(1,32)}$ = 1.643, $p = 0.209$ for Fc; repeated drug administration, $F_{(1,31)}$ = 14.436, $p <$
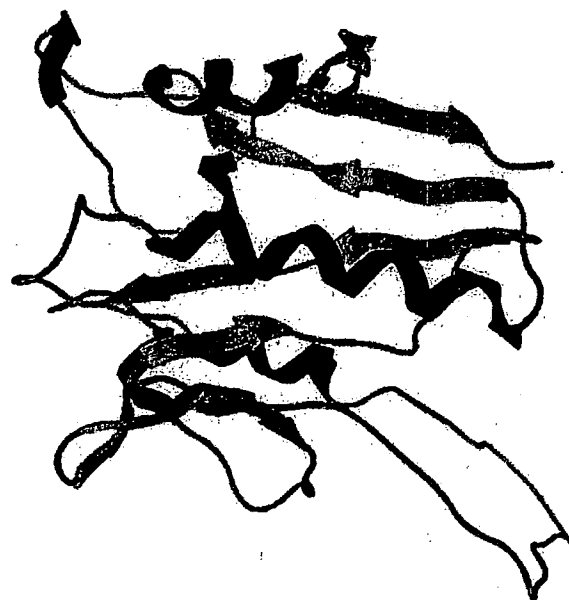
A

```
MHCGPPDMVC  ETKIVATEDH  EALPGAKKDA
LLVAAGAMWP  PLPAAPGPAA  APPPAAGPQP
HGGTGGAGPP  EGRGVCIREF  RAAEQEAARR
IFYDGILERI  PNTAFRGLRQ  HPRTQLLYAL
LAALCFAVTR  SLLLTCLVPA  GLLALRYYYS
RKVILAYLEC  ALHTDMADIE  QYYMKPPGSC
FWVAVLDGNV  VGIVAARAHE  EDNTVELLRM
SVDSRFRGKG  IAKALGRRVL  EFAMLHNYSA
WLGTTAVKV   AAHKLYESLG  FRHMGASDHY
VLPGMTLSLA  ERLFFQVRYH  RYRLQLREE
```

B

C

Figure 1. Characterization of shati. A, The sequence of shati. The red character showed homology modeling of shati. The underlined character showed GCN5-related N-acetyltransferase motif. B, Homology modeling for C-terminal domain of shati. C, Homology modeling and motif analysis of shati. Shati has the sequence of GCAT. Red ribbon, Homology model of shati; sphere, acetyl-CoA analyzed by x-ray crystallography; green ribbon, N-acetyltransferase.
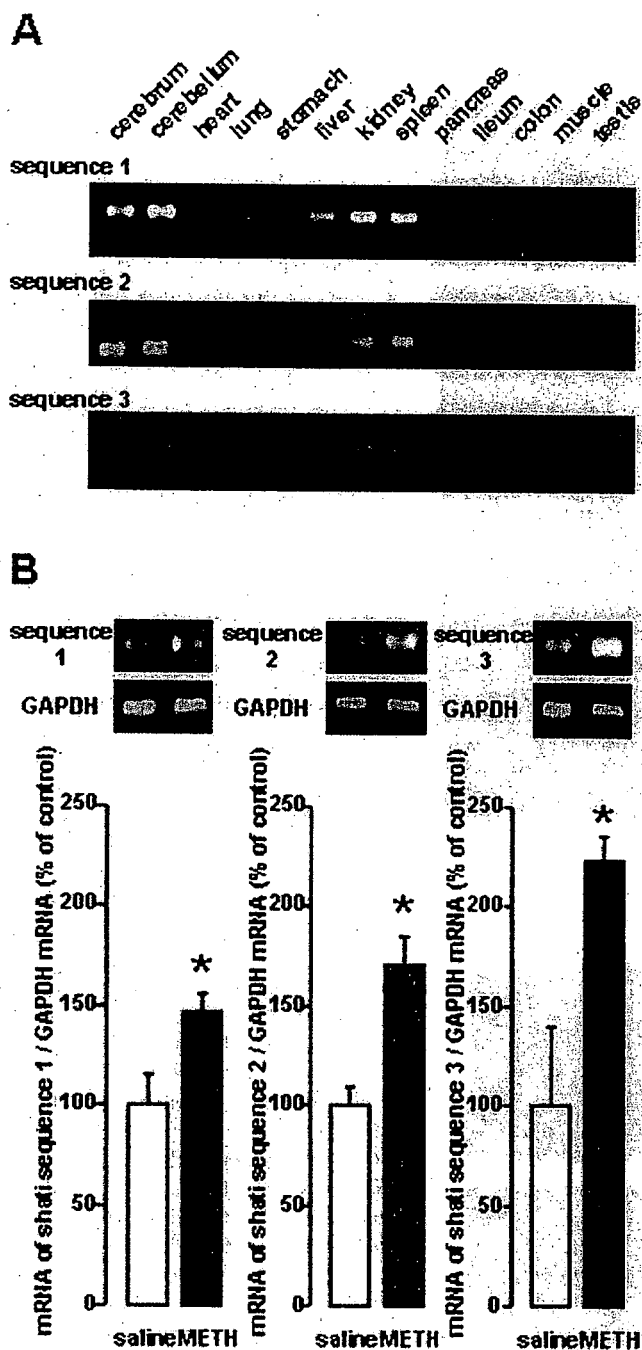
Figure 2. Expression of shati mRNA in the various organs of mice. *A*, RT-PCR analysis of shati in the various organs in mice. Mice were decapitated without any treatment, and the brains were quickly removed. The sets of primers used for PCR are listed in Table 1. *B*, Increase in the production of the three sets of target sequences of shati induced by repeated METH treatment in the NAc of mice. Mice were administered METH (2 mg/kg, s.c.) for 6 d and decapitated 2 h after the last METH treatment. Values are means ± SE ($n = 5$). *$p < 0.05$ versus saline-treated mice. The sets of primers used for PCR are listed in Table 1. To standardize the PCR products, we used primers for glyceraldehyde-3-phosphate dehydrogenase (GAPDH) as the internal control.

Figure 3. METH induced expression of shati mRNA in the brain. *A*, Dose-dependent effect of repeated METH treatment on shati mRNA expression in the NAc. Mice were administered METH (0.3, 1, and 2 mg/kg, s.c.) for 3 d. Mice were decapitated 2 h after the last METH treatment. Values are means ± SE ($n = 8$). *$p < 0.05$ versus saline-treated mice. *B*, Time course changes in the expression of shati mRNA after repeated METH treatment in the NAc. Mice were administered METH (2 mg/kg, s.c.) for 6 d and decapitated 1, 2, 6, 24, and 48 h and 1 week after the last METH treatment. Values are means ± SE ($n = 6-7$). *$p < 0.05$ versus saline-treated mice. *C*, Changes in the expression of shati mRNA in the various brain regions (Fc, NAc, CPu, and Hip) of the mice after single and repeated METH treatment. Mice were administered METH (2 mg/kg, s.c.) for 5 d and challenged with METH (2 mg/kg, s.c.) or saline on day 6. Mice were decapitated 2 h after last treatment of METH (2 mg/kg, s.c.) or saline challenge. Values are means ± SE ($n = 8-10$). *$p < 0.05$ versus saline-treated mice. *D*, The effects of the DA D_1-like receptor antagonist $R(+)$-SCH23390 or D_2-like receptor antagonist raclopride on METH-induced expression of shati mRNA in the NAc. Mice were treated with $R(+)$-SCH23390 (0.1 mg/kg, s.c.) or raclopride (2 mg/kg, s.c.) 30 min before daily METH (2 mg/kg, s.c. for 6 d) treatment. Mice were decapitated 2 h after the last METH treatment. Values are means ± SE ($n = 6-8$). *$p < 0.05$ versus vehicle/saline-treated mice. #$p < 0.05$ versus vehicle/METH-treated mice.

0.01 for NAc; single administration, $F_{(1,31)} = 4.917$, $p < 0.05$ for NAc; repeated drug administration × single administration, $F_{(1,31)} = 10.545$, $p < 0.01$ for NAc; repeated drug administration $F_{(1,32)} = 8.023$, $p < 0.01$ for CPu; single administration, $F_{(1,32)} = 4.833$, $p < 0.05$ for CPu; repeated drug administration × single administration, $F_{(1,32)} = 1.669$, $p = 0.206$ for CPu; repeated drug administration, $F_{(1,32)} = 0.628$, $p = 0.434$ for Hip; single admin-
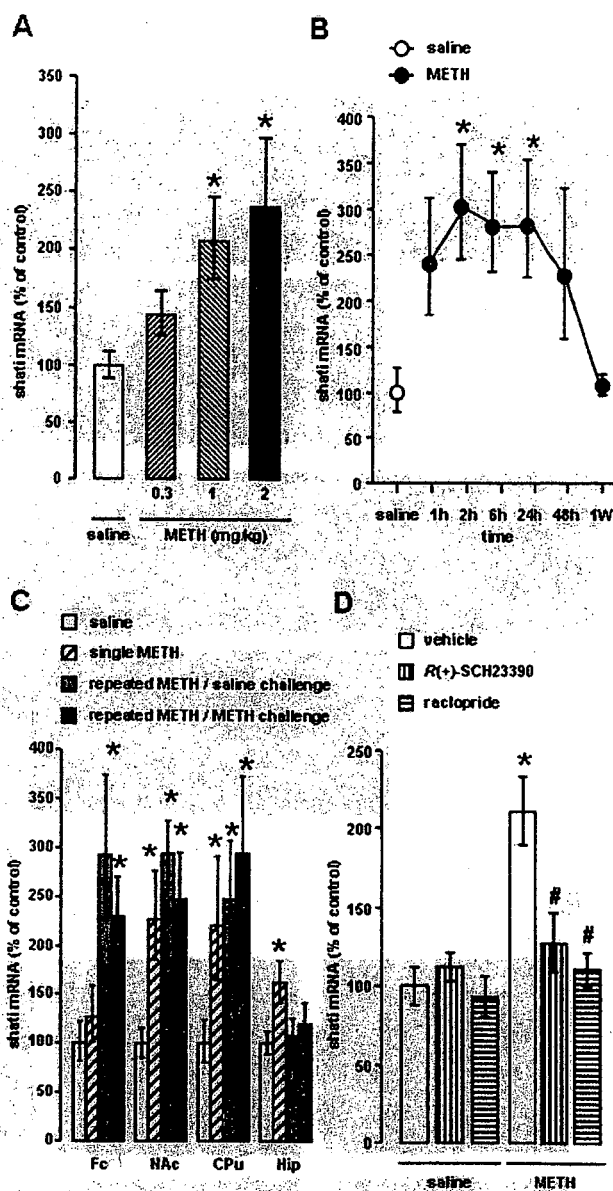
istration, $F_{(1,32)} = 6.464$, $p < 0.05$ for Hip; repeated drug administration × single administration, $F_{(1,32)} = 2.496$, $p = 0.124$ for Hip; two-way ANOVA) (Fig. 3C). The increase caused by METH in the NAc was inhibited by pretreatment with either the DA
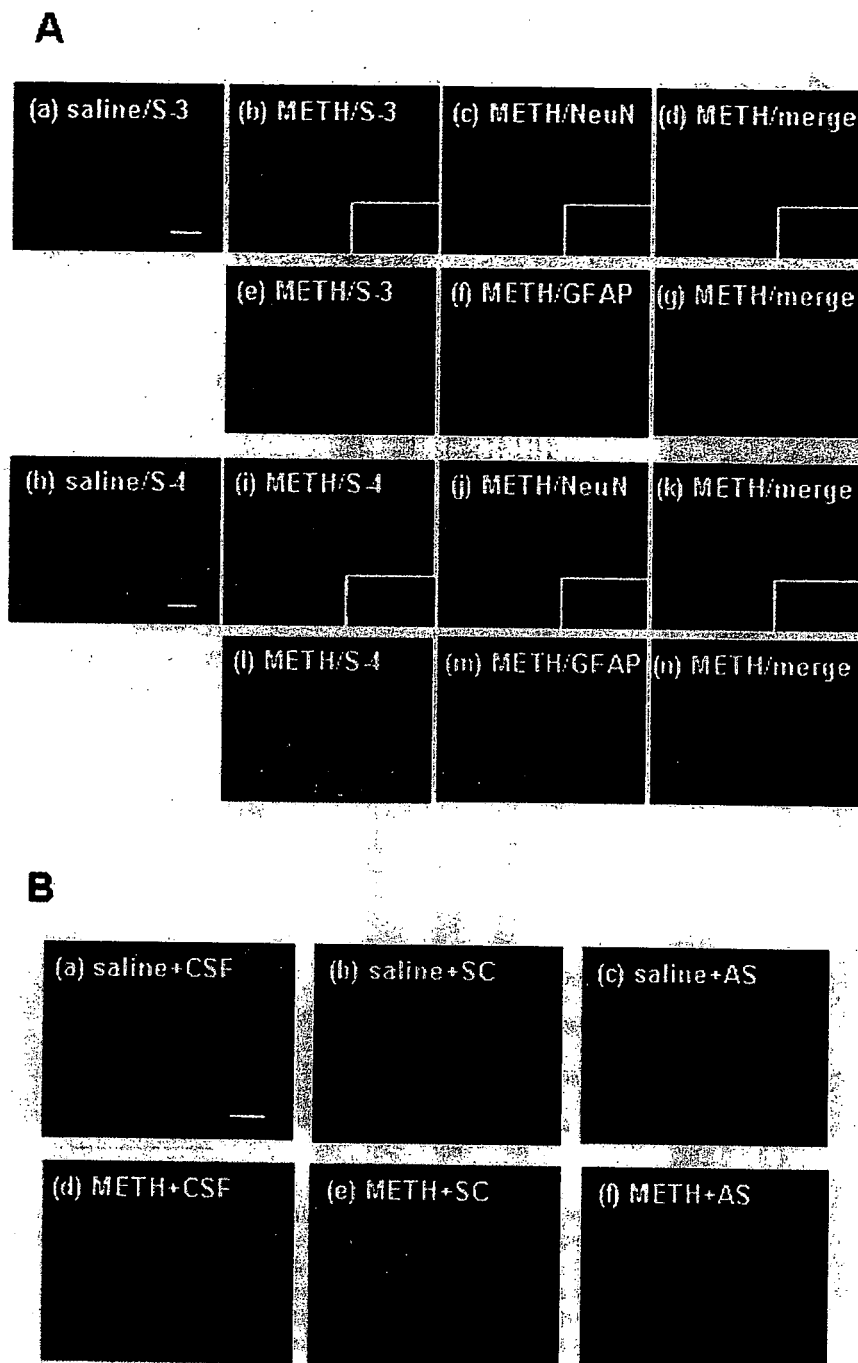
A

B

Figure 4. Immunostaining of shati in the NAc after repeated treatment with METH. Mice were administered METH (2 mg/kg, s.c.) for 6 d and decapitated 24 h after the last treatment. *A*, Double-labeling fluorescence photomicrographs for shati and NeuN or GFAP. The shati-immunopositive cells (green) were colocalized with NeuN-immonopositive cells (red). Double immunostaining for S-3 or S-4 and NeuN in the NAc reveals shati expression in neuronal cells. Scale bars, 20 μm. *B*, Effect of shati-AS on METH-induced increase in shati expression. METH-induced increase in shati expression in the NAc was inhibited by shati-AS. Scale bar, 20 μm.

D_1-like receptor antagonist $R(+)$-SCH23390 (0.1 mg/kg, i.p.) or the D_2-like receptor antagonist raclopride (2 mg/kg, i.p.) (agonist, $F_{(1,34)} = 18.649$, $p < 0.01$; antagonist, $F_{(2,34)} = 5.554$, $p < 0.01$; agonist × antagonist, $F_{(2,34)} = 5.382$, $p < 0.01$; two-way ANOVA) (Fig. 3D), although neither antagonists had an effect on shati mRNA expression in the saline-treated mice. These results indicate that METH induces the expression of shati mRNA in the brain through the activation of both DA D_1 and D_2 receptors.

Localization of shati in the brain of mice treated with METH

There were few shati-immunopositive cells in saline-treated mouse brain (Fig. 4Aa,Ah). METH (2 mg/kg, s.c. for 6 d) increased the number of shati-immunopositive cells in the NAc compared with that in saline-treated mice (Fig. 4A). The shati-immunopositive cells were diminished when the antibodies were absorbed by S-3 or S-4 antigen (data not shown). The shati-immunopositive cells were colocalized with the cells that were immunopositive for NeuN, a neuronal marker, but not for GFAP, an astroglial marker, in the NAc of mice (Fig. 4Ab–A-g,Ai–An). The repeated METH treatment-induced increase in the numbers of shati-immunopositive cells in the NAc was abolished by shati-AS treatment, although shati-SC had no effect (Fig. 4Ba–Bf).

Roles of shati in METH-induced hyperlocomotion and sensitization

To examine the role of shati in the behavioral and neurochemical phenotype in response to METH, we used an AS strategy, which widely used to manipulate gene expression in the brain via intracerebroventricular infusion (Taubenfeld et al., 2001; Bowers et al., 2004). The experimental schedules are shown in Figure 5, A and C. The AS downregulated the expression of shati mRNA in the NAc (Fig. 5B). The increase in the levels of shati mRNA expression evoked by repeated METH treatment in the NAc was significantly and completely abolished by shati-AS, although shati-SC had no effect. Moreover, shati mRNA expression in the NAc of saline-treated mice was also reduced by shati-AS, whereas shati-SC did not affect the expression in saline-treated mice (drug, $F_{(1,42)} = 72.765$, $p < 0.01$; intracerebroventricular treatment, $F_{(2,42)} = 14.104$, $p < 0.01$; drug × intracerebroventricular treatment, $F_{(2,42)} = 0.092$, $p = 0.912$; two-way ANOVA) (Fig. 5B), indicating that shati-AS has an ability to reduce effectively the expression of shati mRNA. We also examined the effect of shati-AS on tPA expression as one of drug-dependence-related other proteins, because tPA–plasmin system potentiates the rewarding and locomotor-stimulating effects of METH, MOR, and nicotine by regulating release of DA (Nagai et al., 2004, 2005a,b, 2006). The increase in the levels of tPA mRNA expression in the NAc was not abolished by shati-AS (drug, $F_{(1,47)} = 62.530$, $p < 0.01$; intracerebroventricular treatment, $F_{(2,47)} = 0.148$, $p = 0.862$; drug × intracerebroventricular treatment, $F_{(2,47)} = 0.803$, $p = 0.454$; two-way ANOVA). Moreover, tPA mRNA expression in the NAc of saline-treated mice was not also reduced by shati-AS, indicating that shati-AS has no ability to

reduce effectively the expression of tPA mRNA (data not shown). Therefore, shati-AS is considered to have no secondary effects.

Repeated METH administration leads to a progressive augmentation of many behavioral effects of the drug (behavioral sensitization). Sensitization is of interest as a model for drug-induced neuroplasticity in neuronal circuits important for addiction. It is well established that the induction of sensitization involves complex neuronal circuitry (Wolf, 1998). In rodent, sensitization is observed as a progressive augmentation of locomotor activity that may relate to an increase in the incentive to obtain drugs (Robinson and Berridge, 1993; Lorrain et al., 2000). There is also evidence of sensitization in human drug users (Satel et al., 1991) and normal subjects (Strakowski and Sax, 1998). Repeated METH treatment (1 and 2 mg/kg, s.c.) for 5 d produced behavioral sensitization [$F_{(2,12)} = 7.404$ for METH (1 mg/kg) plus shati-AS-treated mice; $F_{(2,18)} = 5.593$ for METH (1 mg/kg) plus shati-SC-treated mice; $F_{(2,18)} = 30.917$ for METH (1 mg/kg) plus CSF-treated mice; $F_{(2,12)} = 7.453$ for METH (2 mg/kg) plus shati-AS-treated mice, $F_{(2,12)} = 4.243$ for METH (2 mg/kg) plus shati-SC-treated mice; $F_{(2,15)} = 8.569$ for METH (2 mg/kg) plus CSF-treated mice; $p < 0.05$, one-way ANOVA] (Fig. 5D). As shown in Figure 5D, the shati-AS treatment potentiated the METH (1 mg/kg, s.c.)-induced hyperlocomotion and sensitization compared with shati-SC- or CSF-treated mice (drug, $F_{(2,141)} = 291.696, p < 0.01$; intracerebroventricular treatment, $F_{(2,141)} = 28.223, p < 0.01$; time, $F_{(2,141)} = 17.154, p < 0.01$; drug × intracerebroventricular treatment, $F_{(4,141)} = 12.432, p < 0.01$; drug × time, $F_{(4,141)} = 12.913, p < 0.01$; intracerebroventricular treatment × time, $F_{(4,141)} = 0.156, p = 0.960$; drug × intracerebroventricular treatment × time, $F_{(8,141)} = 0.427, p = 0.903$; three-factor repeated ANOVA), whereas the shati-AS, shati-SC, or CSF treatment had no effect on spontaneous locomotor activity (Fig. 5D). The sensitization was observed on day 10 after challenge administration of METH (0.3 mg/kg, s.c.). Shati-AS-treated mice showed a marked potentiation of METH (0.3 mg/kg, s.c.)-induced sensitization on day 10 compared with shati-SC- or CSF-treated mice ($F_{(2,13)} = 6.974, p < 0.05$, one-way ANOVA), although shati-AS-treated mice did not show a potentiation of METH (2 mg/kg, s.c.)-induced hyperlocomotion and sensitization compared with shati-SC- or CSF-treated mice on days 1–5 (Fig. 5D).
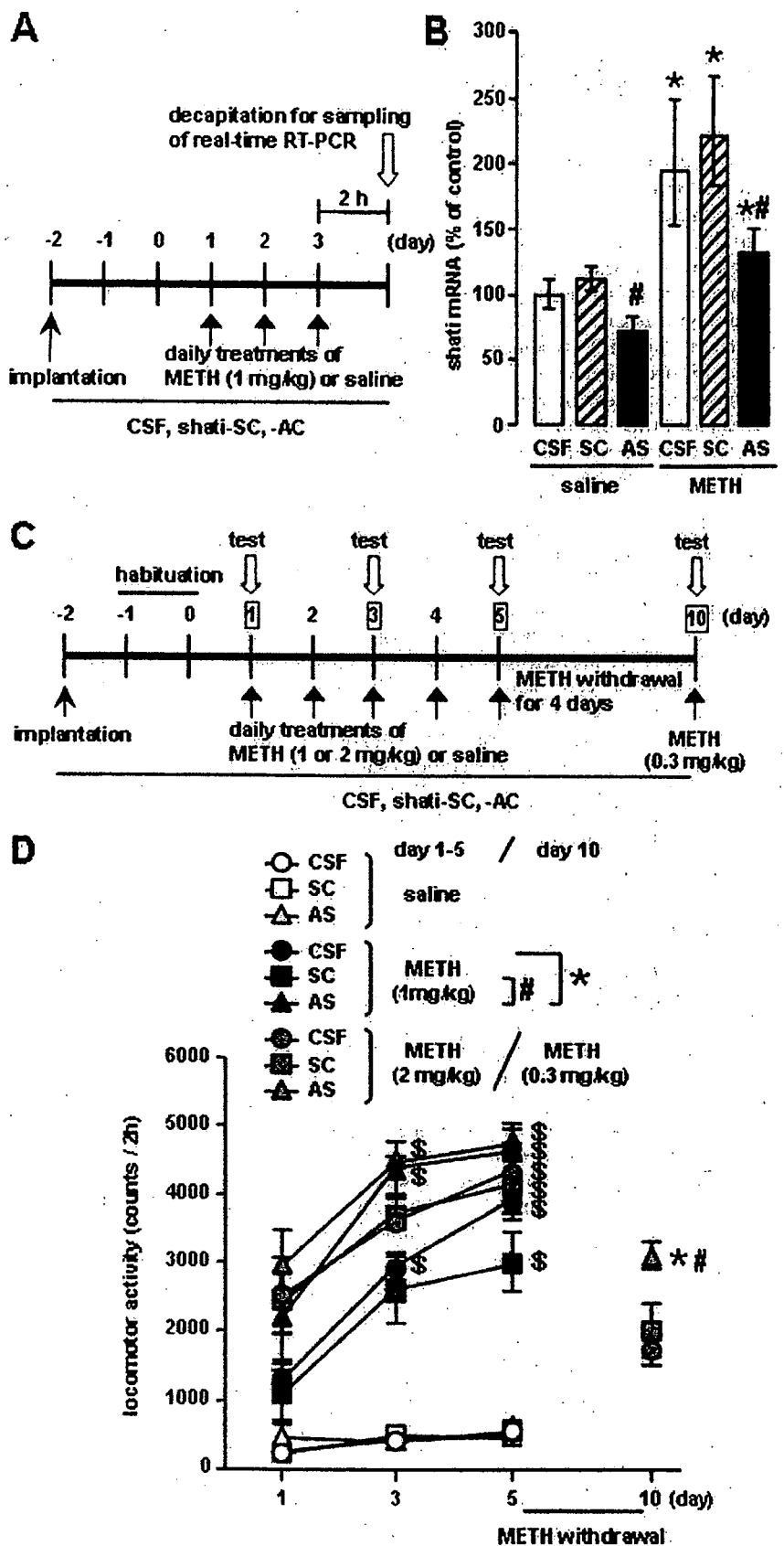
Figure 5. Roles of shati in METH-induced hyperlocomotion and sensitization. An osmotic minipump was used to deliver a continuous infusion of shati-AS (1.8 nmol/6 μl per day), shati-SC (1.8 nmol/6 μl per day), or CSF into the right ventricle (AP −0.5 mm, ML +1.0 mm from bregma, and DV −2.0 mm from the skull). A, Experimental schedule for the real-time RT-PCR using shati-AS. B, Effect of shati-AS on shati mRNA expression. Mice were administered METH (1 mg/kg, s.c.) for 3 d and decapitated 2 h

Roles of shati in METH-induced dopaminergic responses

The pharmacological effects of METH are linked to its capacity to elevate extracellular DA levels by releasing DA from presynaptic nerve terminals and inhibiting its reuptake (Heikkila et al., 1975; Seiden et al., 1993). In addition, METH and the amphetamines redistribute DA from synaptic vesicles to the cytosol and promote reverse transport (Seiden et al., 1993). Therefore, we examined the effect of shati-AS on the METH-induced increase in overflow of DA in the NAc using an *in vivo* microdialysis technique. The experimental schedule is shown in Figure 6A. METH caused a marked increase in overflow of DA in the NAc of the CSF-treated mice on the day 3 (Fig. 6B). The peak of overflow of DA was increased by METH treatment to ~360% of the baseline level in the CSF-treated mice. In shati-AS-treated mice, the METH-induced increase in overflow of DA was significantly potentiated compared with that in the shati-SC- or CSF-treated mice (intracerebroventricular treatment, $F_{(2,14)} = 5.662$, $p < 0.05$; time, $F_{(10,140)} = 35.646$, $p < 0.01$; intracerebroventricular treatment × time, $F_{(20,140)} = 1.927$, $p < 0.05$; repeated ANOVA) (Fig. 6B). The levels of basal DA did not differ among the three groups.

Next, we examined the *in vivo* effect of shati-AS on [^{3}H]DA uptake into synaptosomes in the midbrain. The experimental schedule is shown in Figure 6C. METH decreased [^{3}H]DA uptake compared with the saline-treated mice. In shati-AS-treated mice, the METH-induced decrease in [^{3}H]DA uptake was significantly potentiated compared with that in the shati-SC- or CSF-treated mice. Moreover, [^{3}H]DA uptake in the saline-treated group was also decreased by shati-AS compared with that in the shati-SC- or CSF-treated mice, although shati-SC had no effect on [^{3}H]DA uptake (drug, $F_{(1,40)} = 30.447$, $p < 0.01$; intracerebroventricular treatment, $F_{(2,40)} = 12.576$, $p < 0.01$; drug × intracerebroventricular treatment, $F_{(2,40)} = 0.392$, $p = 0.678$; two-way ANOVA) (Fig. 6D).

We also examined the *in vivo* effect of shati-AS on [^{3}H]DA uptake into synaptic vesicle preparations in the midbrain, because the redistribution of DA from synaptic vesicles to cytoplasmic compartments through interaction with vesicular monoamine transporter-2 has been postulated to be primarily responsible for DA terminal injury by METH or amphetamines (Liu and Edwards, 1997; Uhl, 1998). METH decreased vesicular [^{3}H]DA uptake compared with the saline-treated mice. In shati-AS-treated mice, the METH-induced decrease in vesicular [^{3}H]DA uptake was significantly potentiated compared with that in the shati-SC- or CSF-treated mice. Moreover, [^{3}H]DA uptake in the saline-treated group was also decreased by shati-AS compared with that in the shati-SC- or CSF-treated mice, although shati-SC had no effect on [^{3}H]DA uptake (drug, $F_{(1,42)} = 137.229$, $p < 0.01$; intracerebroventricular treatment, $F_{(2,42)} = 15.087$, $p < 0.01$; drug × intracerebroventricular treatment, $F_{(2,42)} = 0.240$, $p = 0.788$; two-way ANOVA) (Fig. 6E).

Different results were obtained from *in vivo* microdialysis and DA uptake studies, only in the basal conditions. These studies were performed in quite different situations. Living mice were

←

used *in vivo* microdialysis study, and basal overflow of endogenous DA was measured 24 h after the last METH treatment in the NAc (Fig. 6B). Therefore, other factors (other neurotransmitters, neuroplasticity, and neuronal input from other brain regions) might affect basal DA overflow and compensate the dysfunction of DA uptake induced by repeated treatment of METH. Conversely, the experiment of [^{3}H]DA uptake was *ex vivo* study by using the midbrain tissue (Fig. 6D,E). High-concentration and exogenous [^{3}H]DA was used for the investigation of functional changes of DA uptake 1 h after the last METH treatment in the midbrain. The *ex vivo* method could more directly measure the changes of DA uptake in the midbrain, comparing *in vivo* microdialysis study.

Roles of shati in METH-induced conditioned place preference

The effect of shati-AS on METH-induced CPP was examined in a place conditioning paradigm, in which animals learn the association of an environment paired with drug exposure. This paradigm involves sensory perception of external stimuli, association of stimuli, and the approach-inducing actions of a drug, as well as the rewarding effects of a drug. The experimental schedule is shown in Figure 7A. As shown in Figure 7B, METH (0.3 mg/kg, s.c.) produced place preference in mice. In shati-AS-treated mice, the development of METH-induced CPP was significantly potentiated compared with that in the shati-SC- or CSF-treated mice (drug, $F_{(1,46)} = 78.202$, $p < 0.01$; intracerebroventricular treatment, $F_{(2,46)} = 4.950$, $p = 0.011$; drug × intracerebroventricular treatment, $F_{(2,46)} = 5.046$, $p = 0.010$; two-way ANOVA) (Fig. 7B), indicating that downregulation of shati expression was sufficient to confer the enhanced METH-induced CPP. Shati-AS, shati-SC, or CSF treatment had no effect on CPP in saline-treated mice (Fig. 7B, left three columns), suggesting that the procedure in CPP might not reflect anxiolytic actions. These results suggest that shati participates in the repeated METH treatment-induced development of behavioral sensitization and CPP by regulating DA uptake.

Discussion

In the present study, we identified a novel molecule shati from the NAc of mice treated with METH for the first time using the PCR-select cDNA subtraction method, which is a differential and epochal cloning technique.

From motif analysis of shati, shati contained the sequence of GCAT (Fig. 1C). Shati might have physiological action in producing acetylcholine or metabolic action of ATP, because the analysis showed the lowest interactive potential energy of shati with acetyl-CoA or ATP (supplemental Fig. 2, available at www.jneurosci.org as supplemental material). Accordingly, we have to investigate the mechanism by which shati regulates production of acetylcholine or metabolic roles of ATP in subsequent studies.

Because shati expression was detected at high levels in not only the brain regions related to drug dependence but also the liver, kidney, and spleen (Fig. 2A), it is plausible that shati is involved in the regulation of pathophysiological function. Single METH treatment induced the expression of shati mRNA in the NAc and Hip (Fig. 3C). Repeated METH treatment produces an enhancement of the locomotor-stimulating effects of METH (data not shown). Remarkable induction of shati mRNA expression was detected in the Fc, NAc, and CPu of the mice that

showed behavioral sensitization to METH (Fig. 3A–C). There is strong evidence that the dopaminergic system, which projects from the VTA of the midbrain to the NAc and to other forebrain sites, including the Fc, dorsal striatum, and Hip, is a major substrate of reward and reinforcement for both natural rewards and addictive drugs (Di Chiara and Imperato, 1988; Robbins and Everitt, 1996; Wise, 1996a). Therefore, shati may be involved in the rewarding effects and reinforcement of addictive drugs. Because the dopaminergic neuronal system is involved primarily in the pharmacological effects of METH (Melega et al., 1995; Larsen et al., 2002; Sulzer et al., 2005), we examined whether the METH-induced increase in shati mRNA levels is mediated by the activation of dopaminergic neurotransmission. The METH-induced increase in the expression of shati mRNA in the NAc was completely inhibited by pretreatment with the DA D_1-like receptor antagonist $R(+)$-SCH23390 and the DA D_2-like receptor antagonist raclopride (Fig. 3D), suggesting that the activation of DA D_1 and D_2 receptors is attributable to METH-induced expression of shati. Behavioral studies have suggested that both DA D_1 and D_2 receptors mediate reinforcing signals for drug of abuse, because amphetamine-induced CPP and METH-induced sensitization are blocked by either DA D_1-like or D_2-like receptor antagonist (Ujike et al., 1989; Hiroi and White, 1991). Therefore, it likely that activation of DA transmission is necessary for METH-induced shati expression in neurons, in which shati specifically acts (Fig. 4A).

The contribution of dopaminergic transmission to behavioral sensitization and CPP has been well documented (Nakajima et al., 2004; Nagai et al., 2005a,b; Niwa et al., 2007a,b,d). Shati expression was upregulated by repeated administration of METH (Figs. 2B, 3, 4A), and downregulation of shati by AS (Figs. 4B, 5B) led to an elevated synaptic DA concentration in the NAc and major behavioral manifestations in mice: heightened locomotor activity (Fig. 5D), the rate of development of sensitization (Fig. 5D), and CPP (Fig. 7B) responding to METH. Furthermore, downregulation of shati expression by AS (Figs. 4B, 5B) potentiated the effects of METH on overflow of DA in the NAc (Fig. 6B) and DA uptake (Fig. 6D, E). These findings strongly suggest that the overexpression of shati elicited by METH may serve as a homeostatic mechanism that prevents hyperlocomo-
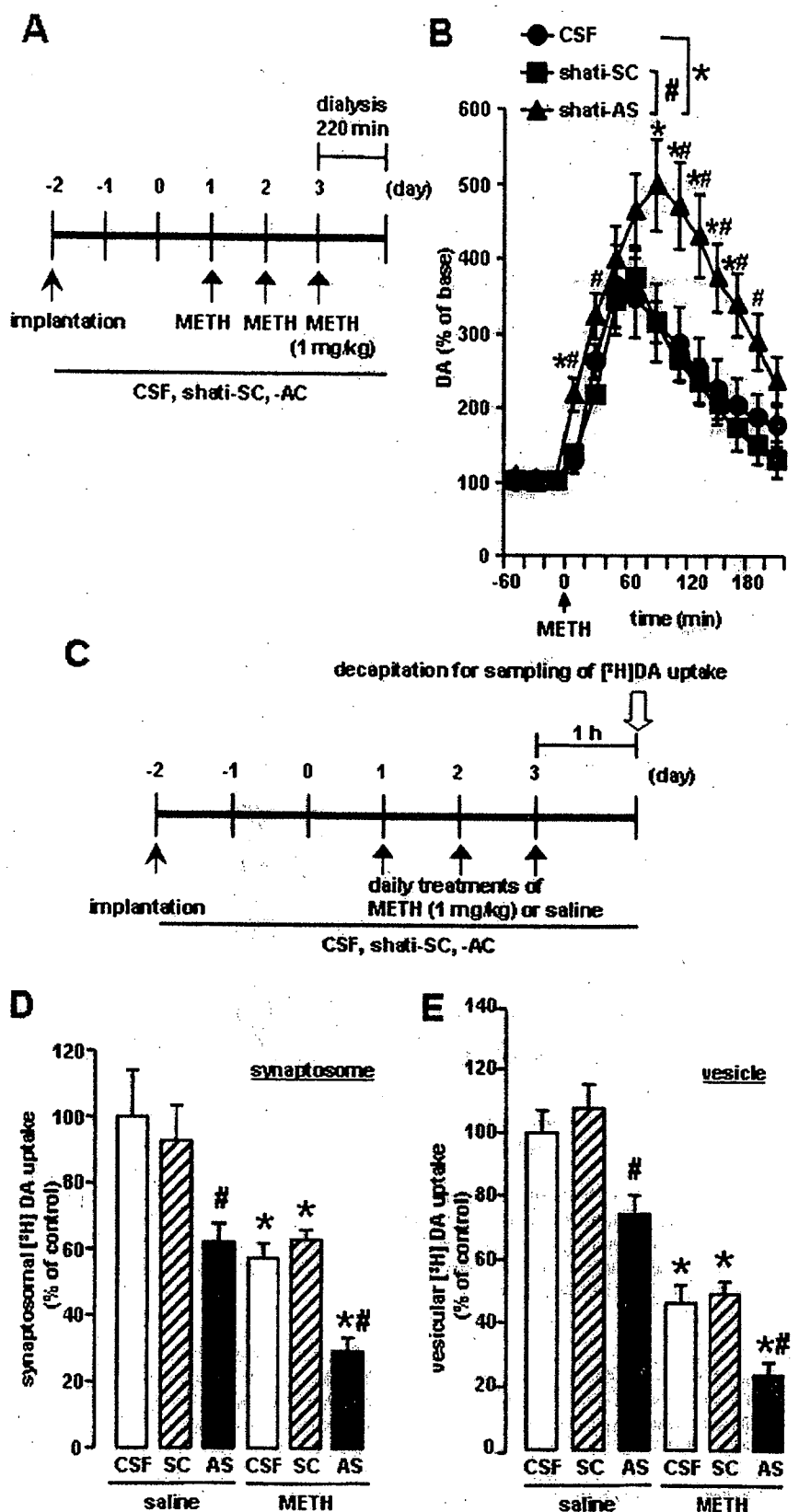
Figure 6. Effects of shati-AS on METH-induced dopaminergic responses. A, Experimental schedule for the measurement of overflow of DA using *in vivo* microdialysis using shati-AS. B, Effect of shati-AS on METH-induced increase in overflow of DA in the NAc. Mice were administered METH (1 mg/kg, s.c.) for 3 d. On day 3, levels of DA were measured in the NAc (AP +1.7 mm, ML −0.8 mm from bregma, and DV −4.0 mm from the skull) for 220 min after METH treatment by *in vivo* microdialysis. Basal levels of DA were 0.30 ± 0.08, 0.31 ± 0.05, and 0.30 ± 0.04 nM for the CSF-treated, shati-SC-treated, and shati-AS-treated mice, respectively. ANOVA with repeated measures revealed significant differences in METH-induced increase in overflow of DA (group,

A

pre-conditioning
test (15 min)

post-conditioning
test (15 min)

habituation

conditioning
(20 min)

0 1 2 [3] 4 5 6 7 8 9 [10](day)

saline   saline   saline

METH   METH   METH (0.3 mg/kg)
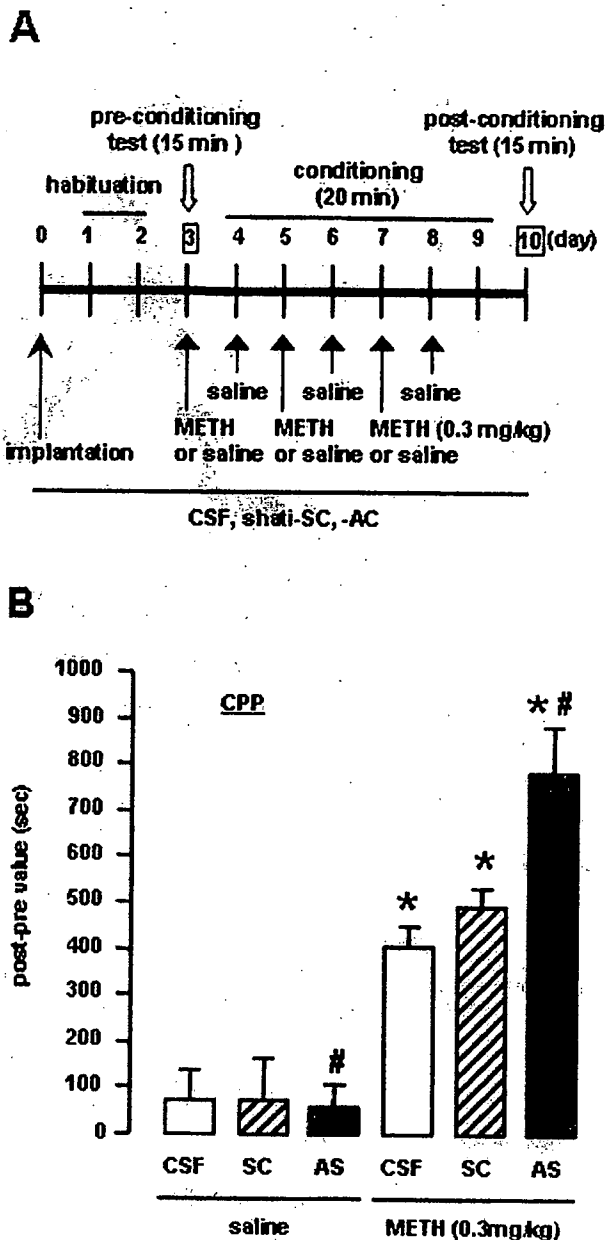or saline or saline or saline

implantation

CSF, shati-SC, -AC

B

Figure 7. Effects of shati-AS on METH-induced conditioned place preference. *A*, Experimental schedule for the conditioned place preference task using shati-AS. *B*, Effect of shati-AS on METH-induced place preference. Mice were administered METH (0.3 mg/kg; s.c.) or saline during the conditioning for place preference. Values are means ± SE ($n = 5$–12). *$p < 0.05$ versus saline-treated mice. #$p < 0.05$ versus shati-SC-treated mice.

←

$F_{(2,14)} = 5.662, p < 0.05$; time, $F_{(10,140)} = 35.646, p < 0.01$; group × time, $F_{(20,140)} = 1.927, p < 0.05$). Values are means ± SE ($n = 5$–6). *$p < 0.05$ versus CSF-treated mice. #$p < 0.05$ versus shati-SC-treated mice. *C*, Experimental schedule for the [³H]DA uptake assay using shati-AS. *D*, Effect of shati-AS on METH-induced decrease of synaptosomal [³H]DA uptake. Mice were administered METH (1 mg/kg, s.c.) for 3 d and decapitated 1 h after the last injection. The synaptosomal [³H]DA uptake was 0.32 ± 0.04, 0.29 ± 0.03, 0.20 ± 0.02, 0.18 ± 0.01, 0.20 ± 0.01, and 0.09 ± 0.01 pmol/mg protein per 4 min for the saline plus CSF-treated, saline plus shati-SC-treated, saline plus shati-AS-treated, METH plus CSF-treated, METH plus shati-SC-treated, and METH plus shati-AS-treated mice, respectively. The final concentration of [³H]DA was 5 nM. Values are means ± SE ($n = 7$–8). *$p < 0.05$ versus saline-treated mice. #$p < 0.05$ versus shati-SC-treated mice. *E*, Effect of shati-AS on METH-induced decrease of vesicular [³H]DA uptake. Mice were administered METH (1 mg/kg, s.c.) for 3 d and decapitated 1 h after the last injection. The vesicular [³H]DA uptake was 3.76 ± 0.25, 4.05 ± 0.29, 2.80 ± 0.20, 1.74 ± 0.21, 1.85 ± 0.14, and 0.90 ± 0.14 pmol/mg protein per 4 min for the saline plus CSF-treated, saline plus shati-SC-treated, saline plus shati-AS-treated, METH plus CSF-treated, METH plus shati-SC-treated, and METH plus shati-AS-treated mice, respectively. The final concentration of [³H]DA was 30 nM. Values are means ± SE ($n = 8$). *$p < 0.05$ versus saline-treated mice. #$p < 0.05$ versus shati-SC-treated mice.

tion, sensitization, and CPP, by promoting plasmalemmal and vesicular DA uptake as well as attenuating the METH-induced increase in overflow of DA in the NAc.

We used METH at the dose of 2 mg/kg for 6 d in the experiments of RT-PCR, real-time RT-PCR, and immunohistochemistry (Figs. 3, 4B–D, 5), because expression of shati was induced in the NAc of mice by METH (2 mg/kg for 6 d), which was detected by using a PCR-select cDNA subtraction method (supplemental Fig. 1, available at www.jneurosci.org as supplemental material). In AS experiments, shati-AS-treated mice tended to show a potentiation of METH (2 mg/kg)-induced hyperlocomotion and sensitization on days 1–5, but there were no statistically significant differences among the three groups (Fig. 5D). The dose–response effects of METH on the locomotor activity may reflect a shift to the left, but these effects were reached the plateau. Conversely, shati-AS-treated mice showed a marked potentiation of METH (1 mg/kg)-induced hyperlocomotion and sensitization on days 1–5 compared with shati-SC- or CSF-treated mice (Fig. 5D). On day 3, the potentiation of the METH-induced hyperlocomotion by shati-AS reached the maximum and plateau. Therefore, in the experiments of AS, we selected METH at the dose of 1 mg/kg for 3 d (Figs. 5B, 6B,D,E). We also confirmed that shati mRNA was increased by METH at the doses of 1 and 2 mg/kg for 3 d (Fig. 3A). Then, in the AS study, we selected METH at the dose of 1 mg/kg to investigate effects of AS.

We selected the time point of 2 h after the last METH treatment for the time when the animals were to be killed in the experiments of RT-PCR and real-time RT-PCR (Figs. 2, 3A,C,D), because expression of shati mRNA showed peak in the NAc of mice 2 h after the last METH treatment (Fig. 3B). We prepared the brain samples 24 h after the last METH treatment for immunohistochemical study (Fig. 4). The levels of shati mRNA in the NAc of mice treated with repeated METH were significantly increased 2, 6, and 24 h after the last METH treatment (Fig. 3B). At 24 h after the METH treatment, both transcription and translation of shati protein could be induced in the brain. Therefore, we considered that 24 h after the METH treatment is the best time point for investigation of shati protein expression.

Changes in mRNA and protein expression caused by drugs are of particular interest. The expression of certain mRNAs and proteins appears to be a compensatory adaptation to excessive DA signaling, which could be biologically significant adaptive mechanisms contributing to dependence. Nevertheless, some proteins play a reverse role. For example, we previously demonstrated that tPA potentiates METH- or MOR-induced rewarding and locomotor-stimulating effects (Nagai et al., 2004, 2005a,b), whereas TNF-α and its inducer inhibit them (Nakajima et al., 2004; Niwa et al., 2007a,b,d). The development of sensitization to amphetamine is prevented when an antibody that neutralized basic fibroblast growth factor (bFGF) is infused into the VTA before amphetamine treatment (Flores et al., 2000). Infusion of brain-derived neurotrophic factor (BDNF) into the NAc enhances the stimulation of locomotor activity by cocaine in rats, whereas the development of sensitization and CPP is delayed in heterozygous BDNF knock-out mice compared with wild-type littermates (Horger et al., 1999; Hall et al., 2003). Infusion of GDNF into the VTA blocks certain biochemical adap-

tations to chronic cocaine treatment (induction of tyrosine hydroxylase, NR1 subunit of NMDA receptors, ΔFosB, and protein kinase A catalytic subunit) as well as cocaine-induced rewarding effects (Messer et al., 2000). Conversely, responses to cocaine are enhanced in rats by intra-VTA infusion of anti-GDNF antibody and in GDNF heterozygous knock-out mice (Messer et al., 2000). A partial reduction in the expression of GDNF potentiates METH self-administration, enhances motivation to take METH, increases vulnerability to drug-primed reinforcement, and prolongs cue-induced reinforcement of extinguished METH-seeking behavior (Yan et al., 2007). cAMP response element-binding protein (CREB) overexpression in the NAc reduces the rewarding properties of cocaine, whereas expression of a dominant-negative form of CREB in this region has the opposite effect (Carlezon et al., 1998; Walters and Blendy, 2001; McClung and Nestler, 2003). Furthermore, FosB mutant mice shows exaggerated locomotor activation in response to initial cocaine exposures as well as robust CPP to a lower dose of cocaine compared with wild-type littermates (Hiroi et al., 1997). Changes in the balance of levels between proaddictive factors, such as bFGF, tPA, and BDNF, and anti-addictive factors, such as TNF-α, GDNF, CREB, and FosB, induced by drugs of abuse seems to be important to the development of drug dependence. In the present study, the facilitation of METH-induced behavioral sensitization in mice with a targeted downregulation of shati highlights the opposing role of shati in drug-dependent behavioral plasticity. Therefore, upregulation of shati expression may represent a homeostastatic response of dopaminergic neurons in the NAc to excessive dopaminergic transmission, resulting in attenuation of hypersensitivity and CPP induced by METH-like drugs. Our findings, together with others, suggest that there are molecules in the brain that normally inhibit the behavioral actions of addictive substances. The mechanism underlying the upregulation of shati caused by METH remains to be elucidated; nevertheless, inhibitory feedback of the excessive DA signaling is likely to be a plausible candidate.

In conclusion, the present study established a functional interaction between shati and METH. Our findings suggest that shati is involved in the development of METH-induced hyperlocomotion, sensitization, and CPP, by promoting plasmalemmal and vesicular DA uptake as well as attenuating the METH-induced increase in overflow of DA in the NAc.

References

Ang E, Chen J, Zagouras P, Magna H, Holland J, Schaeffer E, Nestler EJ (2001) Induction of nuclear factor-κB in nucleus accumbens by chronic cocaine administration. J Neurochem 79:221–224.

Blackshaw S, Harpavat S, Trimarchi J., Cai L, Huang H, Kuo WP, Weber G, Lee K, Fraioli RE, Cho SH, Yung R, Asch E, Ohno-Machado L, Wong WH, Cepko CL (2004) Genomic analysis of mouse retinal development. PLoS Biol 2:E247.

Bowers MS, McFarland K, Lake RW, Peterson YK, Lapish CC, Gregory ML, Lanier SM, Kalivas PW (2004) Activator of G protein signaling 3: a gatekeeper of cocaine sensitization and drug seeking. Neuron 42:269–281.

Carlezon Jr WA, Thome J, Olson VG, Lane-Ladd SB, Brodkin ES, Hiroi N, Duman RS, Neve RL, Nestler EJ (1998) Regulation of cocaine reward by CREB. Science 282:2272–2275.

Cha XY, Pierce RC, Kalivas PW, Mackler SA (1997) NAC-1, a rat brain mRNA, is increased in the nucleus accumbens three weeks after chronic cocaine self-administration. J Neurosci 17:6864–6871.

Christensen AV, Arnt J, Hyttel J, Larsen JJ, Svendsen O (1984) Pharmacological effects of a specific dopamine D-1 antagonist SCH 23390 in comparison with neuroleptics. Life Sci 34:1529–1540.

Diatchenko L, Lau YF, Campbell AP, Chenchik A, Moqadam F, Huang B, Lukyanov S, Lukyanov K, Gurskaya N, Sverdlov ED, Siebert PD (1996) Suppression subtractive hybridization: a method for generating differen-

tially regulated or tissue-specific cDNA probes and libraries. Proc Natl Acad Sci USA 93:6025–6030.

Di Chiara G, Imperato A (1988) Drugs abused by humans preferentially increase synaptic dopamine concentrations in the mesolimbic system of freely moving rats. Proc Natl Acad Sci USA 85:5274–5278.

Douglass J, Daoud S (1996) Characterization of the human cDNA and genomic DNA encoding CART: a cocaine- and amphetamine-regulated transcript. Gene 169:241–245.

Erickson JD, Masserano JM, Barnes EM, Ruth JA, Weiner N (1990) Chloride ion increases [³H]dopamine accumulation by synaptic vesicles purified from rat striatum: inhibition by thiocyanate ion. Brain Res 516:155–160.

Fleckenstein AE, Metzger RR, Wilkins DG, Gibb JW, Hanson GR (1997) Rapid and reversible effects of methamphetamine on dopamine transporters. J Pharmacol Exp Ther 282:834–838.

Flores C, Samaha AN, Stewart J (2000) Requirement of endogenous basic fibroblast growth factor for sensitization to amphetamine. J Neurosci 20:RC55(1–5).

Franklin KBJ, Paxinos G (1997) The mouse brain: in stereotaxic coordinates. San Diego: Academic.

Giros B, Jaber M, Jones SR, Wightman PM, Caron MG (1996) Hyperlocomotion and indifference to cocaine and amphetamine in mice lacking the dopamine transporter. Nature 379:606–612.

Gurskaya NG, Diatchenko L, Chenchik A, Siebert PD, Khaspekov GL, Lukyanov KA, Vagner LL, Ermolaeva OD, Lukyanov SA, Sverdlov ED (1996) Equalizing cDNA subtraction based on selective suppression of polymerase chain reaction: cloning of Jurkat cell transcripts induced by phytohemaglutinin and phorbol 12-myristate 13-acetate. Anal Biochem 240:90–97.

Hall FS, Drgonova J, Goeb M, Uhl GR (2003) Reduced behavioral effects of cocaine in heterozygous brain-derived neurotropic factor (BDNF) knockout mice. Neuropsychopharmacology 28:1485–1490.

Heikkila RE, Orlansky H, Cohen G (1975) Studies on the distinction between uptake inhibition and release of ³H-dopamine in rat brain tissue slices. Biochem Pharmacol 24:847–852.

Hiroi N, White NM (1991) The amphetamine conditioned place preference: differential involvement of dopamine receptor subtypes and two dopaminergic terminal areas. Brain Res 552:141–152.

Hiroi N, Brown JR, Haile CN, Ye H, Greenberg ME, Nestler EJ (1997) FosB mutant mice: loss of chronic cocaine induction of Fos-related proteins and heightened sensitivity to cocaine's psychomotor and rewarding effects. Proc Natl Acad Sci USA 94:10397–10402.

Horger BA, Iyasere CA, Berhow MT, Messer CJ, Nestler EJ, Taylor JR (1999) Enhancement of locomotor activity and conditioned reward to cocaine by brain-derived neurotropic factor. J Neurosci 19:4110–4122.

Koob GF (1992) Drugs of abuse: anatomy, pharmacology and function of reward pathways. Trends Pharmacol Sci 13:177–184.

Koob GF, Sanna PP, Bloom FE (1998) Neuroscience of addiction. Neuron 21:467–476.

Laakso A, Mohn AR, Gainetdinov RR, Caron MG (2002) Experimental genetic approaches to addiction. Neuron 36:213–228.

Larsen KE, Fon EA, Hastings TG, Edwards RH, Sulzer D (2002) Methamphetamine-induced degeneration of dopaminergic neurons involves autophagy and upregulation of dopamine synthesis. J Neurosci 22:8951–8960.

Liu Y, Edwards RH (1997) The role of vesicular transporter proteins in synaptic transmission and neural degeneration. Annu Rev Neurosci 20:125–156.

Lorrain DS, Arnold GM, Vezina P (2000) Previous exposure to amphetamine increases incentive to obtain the drug: long-lasting effects revealed by the progressive ratio schedule. Behav Brain Res 107:9–19.

McClung CA, Nestler EJ (2003) Regulation of gene expression and cocaine reward by CREB and ΔFosB. Nat Neurosci 6:1208–1215.

Melega WP, Williams AE, Schmitz DA, DiStefano EW, Cho AK (1995) Pharmacokinetic and pharmacodynamic analysis of the actions of D-amphetamine and D-methamphetamine on the dopamine terminal. J Pharmacol Exp Ther 274:90–96.

Messer CJ, Eisch AJ, Carlezon Jr WA, Whisler K, Shen L, Wolf DH, Westphal H, Collins F, Russell DS, Nestler EJ (2000) Role for GDNF in biochemical and behavioral adaptations to drugs of abuse. Neuron 26:247–257.

Mizoguchi H, Yamada K, Mizuno M, Mizuno T, Nitta A, Noda Y, Nabeshima T (2004) Regulations of methamphetamine reward by extracellular

signal-regulated kinase 1/2/ets-like gene-1 signaling pathway via the activation of dopamine receptors. Mol Pharmacol 65:1293–1301.

Mizoguchi H, Yamada K, Niwa M, Mouri A, Mizuno T, Noda Y, Nitta A, Itohara S, Banno Y, Nabeshima T (2007) Reduction of methamphetamine-induced sensitization and reward in matrix metalloproteinase-2 and -9-deficient mice. J Neurochem 100:1579–1588.

Nagai T, Yamada K, Yoshimura M, Ishikawa K, Miyamoto Y, Hashimoto K, Noda Y, Nitta A, Nabeshima T (2004) The tissue plasminogen activator-plasmin system participates in the rewarding effect of morphine by regulating dopamine release. Proc Natl Acad Sci USA 101:3650–3655.

Nagai T, Noda Y, Ishikawa K, Miyamoto Y, Yoshimura M, Ito M, Takayanagi M, Takuma K, Yamada K, Nabeshima T (2005a) The role of tissue plasminogen activator in methamphetamine-related reward and sensitization. J Neurochem 92:660–667.

Nagai T, Kamei H, Ito M, Hashimoto K, Takuma K, Nabeshima T, Yamada K (2005b) Modification by the tissue plasminogen activator-plasmin system of morphine-induced dopamine release and hyperlocomotion, but not anti-nociceptive effect in mice. J Neurochem 93:1272–1279.

Nagai T, Ito M, Nakamichi N, Mizoguchi H, Kamei H, Fukakusa A, Nabeshima T, Takuma K, Yamada K (2006) The rewards of nicotine: regulation by tissue plasminogen activator-plasmin system through protease activated receptor-1. J Neurosci 26:12374–12383.

Nakajima A, Yamada K, Nagai T, Uchiyama T, Miyamoto Y, Mamiya T, He J, Nitta A, Mizuno M, Tran MH, Seto A, Yoshimura M, Kitaichi K, Hasegawa T, Saito K, Yamada Y, Seishima M, Sekikawa K, Kim HC, Nabeshima T (2004) Role of tumor necrosis factor-α in methamphetamine-induced drug dependence and neurotoxicity. J Neurosci 24:2212–2225.

Napier TC, Givens BS, Schulz DW, Bunney BS, Breese GR, Mailman RB (1986) SCH23390 effects on apomorphine-induced responses of nigral dopaminergic neurons. J Pharmacol Exp Ther 236:838–845.

Nestler EJ (2001) Molecular basis of long-term plasticity underlying addiction. Nat Rev Neurosci 2:119–128.

Nestler EJ (2002) From neurobiology to treatment: progress against addiction. Nat Neurosci 5:1076–1079.

Niwa M, Nitta A, Shen L, Noda Y, Nabeshima T (2007a) Involvement of glial cell line-derived neurotrophic factor in inhibitory effects of a hydrophobic dipeptide Leu-Ile on morphine-induced sensitization and rewarding effects. Behav Brain Res 179:167–171.

Niwa M, Nitta A, Yamada Y, Nakajima A, Saito K, Seishima M, Shen L, Noda Y, Furukawa S, Nabeshima T (2007b) An inducer for glial cell line-derived neurotrophic factor and tumor necrosis factor-α protects against methamphetamine-induced rewarding effects and sensitization. Biol Psychiatry 61:890–901.

Niwa M, Nitta A, Yamada K, Nabeshima T (2007c) The roles of glial cell line-derived neurotrophic factor, tumor necrosis factor-α, and an inducer of these factors in drug dependence. J Pharmacol Sci, in press.

Niwa M, Nitta A, Yamada Y, Nakajima A, Saito K, Seishima M, Noda Y, Nabeshima T (2007d) Tumor necrosis factor-α and its inducer inhibit morphine-induced rewarding effects and sensitization. Biol Psychiatry, in press.

Noda Y, Miyamoto Y, Mamiya T, Kamei H, Furukawa H, Nabeshima T (1998) Involvement of dopaminergic system in phencyclidine-induced place preference in mice pretreated with phencyclidine repeatedly. J Pharmacol Exp Ther 286:44–51.

Robbins TW, Everitt BJ (1996) Neurobehavioural mechanisms of reward and motivation. Curr Opin Neurobiol 6:228–236.

Robinson TE, Berridge KC (1993) The neural basis of drug craving: an incentive-sensitization theory of addiction. Brain Res Brain Res Rev 18:247–291.

Satel SL, Southwick SM, Gawin FH (1991) Clinical features of cocaine-induced paranoia. Am J Psychiatry 148:495–498.

Schechter MD, Calcagnetti DJ (1998) Continued trends in the conditioned place preference literature from 1992 to 1996, inclusive, with a cross-indexed bibliography. Neurosci Biobehav Rev 22:827–846.

Seiden LS, Sabol KE, Ricaurte GA (1993) Amphetamine: effects on catecholamine systems and behavior. Annu Rev Pharmacol Toxicol 33:639–677.

Strakowski SM, Sax KW (1998) Progressive behavioral response to repeated d-amphetamine challenge: further evidence for sensitization in humans. Biol Psychiatry 44:1171–1177.

Strausberg RL, Feingold EA, Grouse LH, Derge JG, Klausner RD, Collins FS, Wagner L, Shenmen CM, Schuler GD, Altschul SF, Zeeberg B, Buetow KH, Schaefer CF, Bhat NK, Hopkins RF, Jordan H, Moore T, Max SI, Wang J, Hsieh F et al. (2002) Generation and initial analysis of more than 15,000 full-length human and mouse cDNA sequences. Proc Natl Acad Sci USA 99:16899–16903.

Sulzer D, Sonders MS, Poulsen NW, Galli A. (2005) Mechanisms of neurotransmitter release by amphetamines: a review. Prog Neurobiol 75:406–433.

Taubenfeld SM, Milekic MH, Monti B, Alberini CM (2001) The consolidation of new but not reactivated memory requires hippocampal C/EBPβ. Nat Neurosci 4:813–818.

Uhl GR (1998) Hypothesis: the role of dopaminergic transporters in selective vulnerability of cells in Parkinson's disease. Ann Neurol 43:555–560.

Ujike H, Onoue T, Akiyama K, Hamamura T, Otsuki S (1989) Effects of selective D-1 and D-2 dopamine antagonists on development of methamphetamine-induced behavioral sensitization. Psychopharmacology 98:89–92.

Wada R, Tifft CJ, Proia RL (2000) Microglial activation precedes acute neurodegeneration in Sandhoff disease and is suppressed by bone marrow transplantation. Proc Natl Acad Sci USA 97:10954–10959.

Walters CL, Blendy JA (2001) Different requirements for cAMP response element binding protein in positive and negative reinforcing properties of drugs of abuse. J Neurosci 21:9438–9444.

Wang XB, Funada M, Imai Y, Revay RS, Ujike H, Vandenbergh DJ, Uhl GR (1997) rGβ1: a psychostimulant-regulated gene essential for establishing cocaine sensitization. J Neurosci 17:5993–6000.

Wise RA (1996a) Addictive drugs and brain stimulation reward. Annu Rev Neurosci 19:319–340.

Wise RA (1996b) Neurobiology of addiction. Curr Opin Neurobiol 6:243–251.

Wolf ME (1998) The role of excitatory amino acids in behavioral sensitization to psychomotor stimulants. Prog Neurobiol 54:679–720.

Yamada K, Nabeshima T (2004) Pro- and anti-addictive neurotrophic factors and cytokines in psychostimulant addiction: mini review. Ann NY Acad Sci 1025:198–204.

Yan Y, Yamada K, Niwa M, Nagai T, Nitta A, Nabeshima T (2007) Enduring vulnerability to reinstatement of methamphetamine-seeking behavior in glial cell line-derived neurotrophic factor mutant mice. FASEB J, in press.

Zachariou V, Bolanos CA, Selley DE, Theobald D, Cassidy MP, Kelz MB, Shaw-Lutchman T, Berton O, Sim-Selley LJ, Dileone RJ, Kumar A, Nestler EJ (2006) An essential role for ΔFosB in the nucleus accumbens in morphine action. Nat Neurosci 9:205–211.

Carvedilol increases ciclosporin bioavailability by inhibiting P-glycoprotein-mediated transport

Katsuo Amioka, Takafumi Kuzuya, Hideyuki Kushihara,
Masayuki Ejiri, Atsumi Nitta and Toshitaka Nabeshima

Department of
Neuropsychopharmacology and
Hospital Pharmacy, Nagoya
University School of Medicine, 65
Tsuruma-cho, Showa-ku, Nagoya
466-8560, Japan

Katsuo Amioka, Takafumi Kuzuya,
Masayuki Ejiri, Atsumi Nitta,
Toshitaka Nabeshima

Clinical Pharmacy, College of
Pharmacy, Kinjogakuin
University, 2-1723 Omori,
Moriyama-ku, Nagoya 463-8521,
Japan

Katsuo Amioka

Department of Hospital
Pharmacy, Japanese Red Cross
Nagoya First Hospital, 3-35
Mitishita-cho, Nakamura-ku,
Nagoya, 453-8511, Japan

Hideyuki Kushihara

Correspondence:
T. Nabeshima, Department
of Neuropsychopharmacology
and Hospital Pharmacy, Nagoya
University School of Medicine,
65 Tsuruma-cho, Showa-ku,
Nagoya 466-8560, Japan. E-mail:
tnabeshi@med.nagoya-u.ac.jp

Abstract

Carvedilol is often used to treat hypertension and for prophylaxis in vascular sclerosis in renal transplant recipients, who require concomitant treatment with ciclosporin. However, there are few reports regarding the pharmacokinetic interactions between carvedilol and ciclosporin. We have investigated the potential effects of carvedilol on the pharmacokinetics of ciclosporin, and examined the inhibitory effects of carvedilol on P-glycoprotein-mediated transcellular transport using Caco2 cells. Ciclosporin alone or with carvedilol was orally or intravenously administered to rats. The oral administration of carvedilol ($10 \, \text{mg kg}^{-1}$) with ciclosporin ($10 \, \text{mg kg}^{-1}$) increased the whole blood concentration of ciclosporin. When ciclosporin ($3 \, \text{mg kg}^{-1}$) was intravenously administered with carvedilol ($3 \, \text{mg kg}^{-1}$), there was no difference in the whole blood ciclosporin concentration between administration with and without carvedilol. Co-administration with carvedilol increased ciclosporin bioavailability from 33% to 70%. In Caco2 cells, carvedilol caused a concentration-dependent increase in the intracellular accumulation of ciclosporin, and its effect was comparable with that of verapamil. Carvedilol considerably raised the concentration of ciclosporin in the blood and this interaction was associated with the absorption phase of ciclosporin. This interaction was caused by the inhibition of P-glycoprotein-mediated transport by carvedilol in the intestine.

Introduction

Carvedilol is a nonselective β-blocking agent which has vasodilating properties that are attributed mainly to its blocking activity at α_1-receptors. Since carvedilol is used in the treatment of mild to moderate hypertension and does not affect renal perfusion and filtration, it can be given to renal transplant recipients (Heitmann et al 2002). In addition, carvedilol has been found to inhibit the proliferation and migration of vascular smooth muscle cells (Patel et al 1995; Park et al 2006). This pharmacological effect may be useful for renal transplant recipients because chronic rejection is associated with the abnormal proliferation and migration of vascular smooth muscle, and fibrosis is a common feature of transplant vascular sclerosis (Ishii et al 2005). For these reasons, there are many cases where carvedilol and immunosuppressive agents could and should be used concomitantly.

Carvedilol, when absorbed orally, is extensively metabolized and then excreted primarily into the bile (Gehr et al 1999). Ciclosporin, the principal immunosuppressant used in organ transplant patients and employed to treat a variety of autoimmune diseases, is extensively metabolized in the liver and eliminated mainly by biliary excretion (Lindholm 1991). Both drugs have been shown to be transported by P-glycoprotein, which plays a significant role in the oral absorption and excretion of xenobiotics (Saeki et al 1993; Kakumoto et al 2003). These points should be taken into account when considering factors affecting drug–drug interactions, and specifically the pharmacokinetics of ciclosporin. Indeed, we have had firsthand experience of increased ciclosporin blood levels after administering carvedilol concomitantly to a renal transplant patient: the patient's AUC_{0-4}/dose increased 24%. However, there are few reports describing the pharmacokinetic interaction between carvedilol and ciclosporin, and the mechanisms behind the interaction are not clear.

The purpose of this study was to examine the potential effects of carvedilol on the pharmacokinetics of ciclosporin. Furthermore, the inhibitory effects of carvedilol on

P-glycoprotein-mediated transport were investigated using a human colon adenocarcinoma cell line.

Materials and Methods

Materials

Ciclosporin and carvedilol were kindly provided by Novartis Pharma K. K. (Tokyo, Japan) and Daiichi Pharmaceutical Co. Ltd (Tokyo, Japan), respectively. Verapamil, Dulbecco's modified Eagle medium (DMEM), fetal bovine serum, Triton X-100, and trypsin were purchased from Sigma-Aldrich (St Louis, MO). HEPES, penicillin, streptomycin, and nonessential amino acids were purchased from Gibco BRL (Grand Island, NY). All other chemicals used were of the highest purity available.

Animal study

All experiments were performed in accordance with the Guidelines for Animal Experiments of Nagoya University Graduate School of Medicine. Male Wistar rats (280–320 g; Japan SLC Inc., Shizuoka, Japan) were used for the pharmacokinetic study. Although food was withdrawn overnight before the experiment, rats were always allowed free access to water. One day before drug administration, the rats were anaesthetized with an intraperitoneal injection of sodium pentobarbital (25 mg kg^{-1}). A silastic catheter was inserted into the right jugular vein to allow the collection of blood samples and as a route for intravenous administration. Doses of ciclosporin either alone or with carvedilol were orally (ciclosporin 10 mg kg^{-1}; carvedilol 10 mg kg^{-1}) or intravenously (ciclosporin 3 mg kg^{-1}; carvedilol 3 mg kg^{-1}) administered. These dosage adjustments were required due to the poor absorption of ciclosporin (27±18% (Ptachcinski et al 1985)). Oral administration was accomplished by inserting a water-lubricated curved blunt stainless-steel catheter into the oesophagus. Blood samples were collected using heparinized syringes at 1, 2, 4, 6, 8, and 12 h post-dose and were analysed for ciclosporin using a fluorescence polarization immunoassay with a TDX analyser (Abbott Laboratories, Chicago, IL). Ciclosporin blood concentrations were fitted to a one-compartment model with first-order absorption and elimination using Prism 4 for Windows software (GraphPAD Software Inc, San Diego, CA).

Cell culture and intracellular accumulation study

P-glycoprotein function was studied in the epithelial layer of a human colon adenocarcinoma cell line, Caco-2, which demonstrates a P-glycoprotein-dependent intestinal absorptive cell phenotype. Caco-2 cells at passage 40 were obtained from Riken Gene Bank (Tsukuba, Japan). They were cultured in DMEM containing 10% fetal bovine serum, 100 U mL^{-1} penicillin, 100 μg mL^{-1} streptomycin, and 100 μM nonessential amino acids. The adhesive cells were harvested at 80% confluence by exposure to a trypsin-EDTA solution (0.25% trypsin and 0.02% EDTA in a phosphate-buffered solution).

Intracellular accumulation was studied according to a procedure described by Zhu et al (2006). In brief, Caco-2 cells were seeded at a density of 1×10^5 cells mL^{-1}/well in 24-well plates, and the culture medium was changed every two days until the experiment was initiated. After reaching confluence, Caco-2 cells were pre-incubated at 37°C for 30 min with serum-free DMEM containing 25 mM HEPES, pH 7.4. Ciclosporin and either carvedilol or verapamil were added to the culture medium to a final concentration of 0.1 μM for ciclosporin, and 0.02, 0.2, 0.6, 2 or 20 μM for carvedilol and verapamil. The solution contained no more than 0.1% dimethyl sulfoxide, and was discarded after 90-min incubation. The cells were washed three times with ice-cold phosphate-buffered saline and permeabilized with a 1% Triton X-100-containing buffer. The ciclosporin concentrations in the buffer were analysed using the method described above but with a different calibration curve. The amount of ciclosporin in each sample was standardized, with the protein content determined using a BCA protein assay kit (Pierce, Rockford, IL). The degree of inhibition observed at the different carvedilol or verapamil concentrations was estimated based on a 50% inhibitory concentration (IC50) determined with an inhibitory sigmoid E_{max} model using non-linear regression curve fitting; the results were analysed using Prism 4 for Windows software (GraphPAD Software Inc, San Diego, CA).

Statistical analysis

All data are presented as the mean±s.d. The individual differences of ciclosporin concentrations with and without carvedilol at each sampling time were performed using a Mann–Whitney U-test. The differences of each pharmacokinetic parameter were also established using the same test, with $P < 0.05$ being taken as significant. All statistical analyses were performed with StatView 4.5 (Abacus Concepts Inc., Berkeley, CA).

Results

Pharmacokinetic study

Figure 1 shows the whole blood concentration–time curves of ciclosporin after oral (ciclosporin 10 mg kg^{-1}, Figure 1A) and intravenous (ciclosporin 3 mg kg^{-1}, Figure 1B) administration, with and without carvedilol (i.v. 3 mg kg^{-1}; p.o. 10 mg kg^{-1}). Co-administration of carvedilol significantly ($P < 0.05$) increased the whole blood concentration of ciclosporin following oral administration. When ciclosporin was intravenously administered with carvedilol, there was no difference in the whole blood ciclosporin concentration to when administered without carvedilol. The pharmacokinetic parameters of ciclosporin with and without carvedilol are shown in Table 1. Co-administration of carvedilol resulted in a decrease in clearance (CL) and a 2-fold increase in AUC and C_{max} compared with administration of ciclosporin alone when the drugs were taken orally. The pharmacokinetic parameters (AUC and CL) were not altered when carvedilol was administered intravenously. Since the increase in AUC was linear with ciclosporin dose, co-administration with carvedilol showed
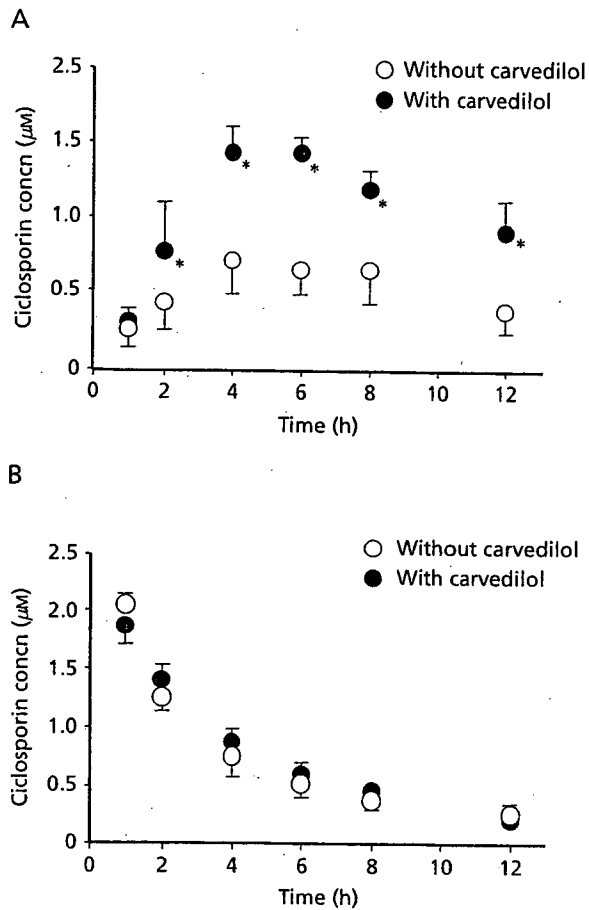
A

B

Figure 1 Whole blood concentration–time curves of ciclosporin after (A) 10 mg kg^{-1} orally administered with or without carvedilol or (B) 3 mg kg^{-1} intravenously administered with or without carvedilol. Each point represents the mean ± s.d. of four rats. *$P < 0.05$, significantly different from administration without carvedilol.

Table 1 Effect of carvedilol on pharmacokinetic parameters of ciclosporin

Parameter	Oral administration		Intravenous administration	
	Control	Carvedilol	Control	Carvedilol
AUC (μM h)	9.8 ± 2.7	23.6 ± 5.7	9.1 ± 1.7	10.2 ± 1.4
		$P < 0.01$		$P = 0.17$
k_a (h^{-1})	0.17 ± 0.04	0.21 ± 0.06		
		$P = 0.38$		
k_{el} (h^{-1})	0.17 ± 0.06	0.17 ± 0.03	0.27 ± 0.08	0.23 ± 0.01
		$P = 0.46$		$P = 0.17$
Vd/F (L kg^{-1})	4.25 ± 0.51	2.25 ± 0.13		
		$P < 0.01$		
Vd (L kg^{-1})			1.00 ± 0.40	1.10 ± 0.09
				$P = 0.47$
CL/F (L h^{-1} kg^{-1})	0.71 ± 0.15	0.39 ± 0.03		
		$P < 0.01$		
CL (L h^{-1} kg^{-1})			0.27 ± 0.13	0.25 ± 0.03
				$P = 0.56$
C_{max} (μM)	0.72 ± 0.10	1.42 ± 0.12		
		$P < 0.01$		

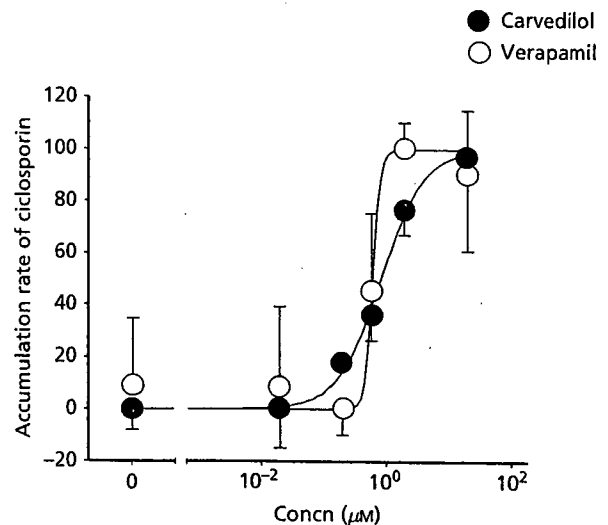**Figure 2** Concentration-dependent accumulation rate of 0.1 μM ciclosporin by carvedilol and verapamil in Caco-2 cells. The IC50 values of carvedilol and verapamil were 0.83 and 0.62 μM, respectively. Each point represents the mean ± s.d. of four data points.

an increase in bioavailability of ciclosporin from 32.6% to 70.1%. The elimination rate constants were not altered by carvedilol administered either orally or intravenously. These results suggested that the increase in the AUC and C_{max} of ciclosporin induced by carvedilol via the oral route was mainly due to enhanced absorption of ciclosporin in the gastrointestinal tract, and not to inhibited elimination via the biliary tract or to hepatic metabolism.

Intracellular accumulation study

Ciclosporin is a substrate of P-glycoprotein and is transported across Caco-2 cell membranes. Since Caco-2 cells exhibit features typical of intestinal epithelial cells (Sambuy et al 2005), these cells have been used widely as a standard model for intestinal efflux, and for investigating the mechanisms of absorption of several classes of drugs. We evaluated the inhibitory effect of carvedilol on the efflux of ciclosporin using the intracellular accumulation study. As shown in Figure 2, the accumulation of ciclosporin was markedly increased in the presence of carvedilol, the effects of which

were dependent on concentration. This concentration-dependent accumulation of ciclosporin was also found with verapamil in Caco-2 cells. The IC50 value of carvedilol (0.831 μM) was comparable with that of verapamil (0.616 μM).

Discussion

Padi & Chopra (2002) reported that ciclosporin induced oxidative stress and that the resultant renal dysfunction was prevented by carvedilol, which has potent antioxidative effects. These results indicated that co-administration of carvedilol

with ciclosporin was useful not only for the treatment of hypertension and the inhibition of muscular smooth muscle cell proliferation, but also for the prevention of ciclosporin-induced nephrotoxicity. However, there are few clinical reports regarding the interaction between ciclosporin and carvedilol, and the precise mechanism of this interaction has yet to be elucidated. Therefore, we have investigated the effect of carvedilol on the pharmacokinetics of ciclosporin in rats and in the Caco-2 cell line (which expresses P-glycoprotein). Previous reports indicated that blood levels of ciclosporin increased when carvedilol was introduced, and thus the dose of ciclosporin had to be decreased by 20% (Kaijser et al 1997) or 10% (Bader et al 2005). Kaijser et al (1997) speculated that cytochrome P450 enzymes contributed to this interaction. Indeed, ciclosporin is metabolized by CYP3A4, which plays a dominant role in the metabolic elimination of many drugs (Lamba et al 2002). Drugs which are substrates of CYP3A4, including calcium channel blockers, macrolide antibiotics, and antifungal azoles, have been shown to clinically increase the concentrations of ciclosporin in blood (Guan et al 1996; Koselj et al 1994). Carvedilol undergoes extensive metabolism by CYP2D6, CYP3A4, CYP1A2, CYP2E1 and CYP2C9, while CYP2D6 is the rate-limiting enzyme for the overall disposition (Gehr et al 1999; Graff et al 2001). CYP3A4 has a minor influence on the disposition of carvedilol, because the increase in metabolic clearance after treatment with rifampicin, which markedly induced the expression of CYP3A4, contributed only slightly to the increase in total body clearance (Giessmann et al 2004). Therefore, it was presumed that the probability of a drug–drug interaction dependent on CYP3A4 was unlikely. Figure 1B indicates that carvedilol did not interact with ciclosporin during the elimination phase, indicating that the absorption of ciclosporin was increased by carvedilol, as shown in Figure 1A.

The activity of cytochrome P450 affects not only drug elimination, but also the bioavailability of many drugs. Several studies have shown that intestinal CYP3A4 was responsible for the first pass metabolism of orally administered ciclosporin (Gomez et al 1995; Wu et al 1995). However, if carvedilol were to inhibit intestinal CYP3A4, it would also inhibit liver CYP3A4 activity. Therefore, it was quite unlikely that this was the mechanism behind the interaction. On the other hand, Bader et al (2005) suggested that carvedilol influenced ciclosporin levels through its effects on P-glycoprotein in cardiac transplant recipients. We designed an in-vitro study to evaluate the inhibitory effects of carvedilol on ciclosporin transport. Several in-vitro models have been proposed to determine the inhibitory effect or substrate specificity of P-glycoprotein. In this study, we examined the inhibitory effects of carvedilol and verapamil on the intracellular uptake of the P-glycoprotein substrate ciclosporin in Caco-2 cells. The Caco-2 cell line has been used extensively as a model of the intestinal barrier and absorptive properties of the intestinal mucosa. Caco-2 cells express many kinds of transporter proteins such as multidrug resistance-associated proteins, P-glycoprotein, peptide transporters, organic anion transporters, and organic cation transporters (Katsura & Inui 2003). Previous reports indicated that the pharmacokinetics of ciclosporin were related to the expression level of enterocyte P-glycoprotein in renal transplant

patients (Lown et al 1997). Additionally, the basolateral to apical transport of ciclosporin is much greater across human MDR1 cDNA-transfected porcine kidney epithelial LLC-PK1 cells than in LLC-PK1 cells (Adachi et al 2001). Therefore, P-glycoprotein is mainly responsible for the cellular extrusion of ciclosporin. Verapamil is also a well established probe that is routinely used to identify compounds that have the potential to inhibit P-glycoprotein.

Carvedilol has been found to be a substrate of P-glycoprotein, which can be considered as another mechanism of drug–drug interaction (Kakumoto et al 2003; Bart et al 2005). Kakumoto et al (2003) indicated that carvedilol inhibited the treatment of anticancer drugs mediated by P-glycoprotein, and that the inhibitory effect was similar to that of verapamil. The results of our study using Caco-2 cells also showed that carvedilol inhibited the transport of ciclosporin mediated by P-glycoprotein, and that this inhibitory effect was comparable with that of verapamil. After long-term oral administration of carvedilol (25 mg/day) to healthy subjects, the peak plasma concentration in extensive metabolizers and poor metabolizers of CYP2D6 was nearly 0.1 and 0.15 μM, respectively (Giessmann et al 2004). This concentration was almost the 20% inhibitory concentration for the transport of ciclosporin obtained in this study. Therefore, there is a possibility of interaction between ciclosporin and carvedilol in the clinical setting.

Kakumoto et al (2003) speculated that the antioxidative effect of carvedilol caused the inhibitory effect on P-glycoprotein-mediated transport. Indeed, it has been reported that high levels of reactive oxygen species, resulting in severe cellular oxidative stress, increased the expression of MDR1 genes (Ziemann et al 1999). However, this was unlikely because in our study only 90-min incubation with carvedilol inhibited the transport of ciclosporin across Caco-2 cells, and a previous study demonstrated a significant increase in mdr1b mRNA expression after two days of treatment with H_2O_2 (Ziemann et al 1999). Further study is needed to clarify the mechanism.

Ciclosporin is also known to inhibit P-glycoprotein-mediated transport (Chiou et al 2002). Carvedilol is not usually trapped in the brain because P-glycoprotein in the blood–brain barrier extrudes carvedilol from the brain. Bart et al (2005) indicated that the amount of carvedilol taken up in the rat brain was increased after pretreatment with ciclosporin. Although we did not monitor the concentration of carvedilol in blood in this study, there is a possibility that carvedilol blood concentration, and also the distribution of carvedilol in the brain, could be increased after co-treatment with ciclosporin. There have been no studies regarding the interaction between carvedilol and ciclosporin in man which focus on carvedilol, but we should be aware of such cases and monitor clinical symptoms closely.

Conclusion

Co-administration with carvedilol increased ciclosporin bioavailability. By using Caco-2 cells, we found that carvedilol caused a concentration-dependent increase in the intracellular accumulation of ciclosporin, and its effect was comparable with that of verapamil. This study has shown that carvedilol

considerably raised the concentration of ciclosporin in blood, and that this interaction was associated with the absorption phase of ciclosporin caused by the inhibition of P-glycoprotein-mediated transport by carvedilol in the intestine.

References

Adachi, Y., Suzuki, H., Sugiyama, Y. (2001) Comparative studies on in vitro methods for evaluating in vivo function of MDR1 P-glycoprotein. *Pharm. Res.* **18**: 1660–1668

Bader, F. M., Hagan, M. E., Crompton, J. A., Gilbert, E. M. (2005) The effect of β-blocker use on cyclosporine level in cardiac transplant recipients. *J. Heart Transplant* **24**: 2144–2147

Bart, J., Dijkers, E. C., Wegman, T. D., de Vries, E. G., van der Graaf, W. T., Groen, H. J., Vaalburg, W., Willemsen, A. T., Hendrikse, N. H. (2005) New positron emission tomography tracer [(11)C]carvedilol reveals P-glycoprotein modulation kinetics. *Br. J. Pharmacol.* **145**: 1045–1051

Chiou, W. L., Wu, T. C., Ma, C., Jeong, H. Y. (2002) Enhanced oral bioavailability of docetaxel by coadministration of cyclosporine: quantitation and role of P-glycoprotein. *J. Clin. Oncol.* **20**: 1951–1952

Gehr, T. W. B., Tenero, D. M., Boyle, D. A., Qian, Y., Sica, D. A., Shusterman, N. H. (1999) The pharmacokinetics of carvedilol and its metabolites after single and multiple dose oral administration in patients with hypertension and renal insufficiency. *Eur. J. Clin. Pharmacol.* **55**: 269–277

Giessmann, T., Modess, C., Hecker, U., Zschiesche, M., Dazert, P., Kunert-Keil, C., Warzok, R., Engel, G., Weitschies, W., Cascorbi, I., Kroemer, H. K., Siegmund, W. (2004) CYP2D6 genotype and induction of intestinal drug transporters by rifampin predict presystemic clearance of carvedilol in healthy subjects. *Clin. Pharmacol. Ther.* **75**: 213–222

Gomez, D. Y., Wacher, V. J., Tomlanovich, S. J., Hebert, M. F., Benet, L. Z. (1995) The effects of ketoconazole on the intestinal metabolism and bioavailability of cyclosporine. *Clin. Pharmacol. Ther.* **58**: 15–19

Graff, D. W., Williamson, K. M., Pieper, J. A., Carson, S. W., Adams, K. F., Cascio, W. E., Patterson, J. H. (2001) Effect of fluoxetine on carvedilol pharmacokinetics, CYP2D6 activity, and autonomic balance in heart failure patients. *J. Clin. Pharmacol.* **41**: 97–106

Guan, D., Wang, R., Lu, J., Wang, M., Xu, C. (1996) Effects of nicardipine on blood cyclosporine levels in renal transplant patients. *Transplant. Proc.* **28**: 1311–1312

Heitmann, M., Davidsen, U., Stokholm, K. H., Rasmussen, K., Burchardt, H., Petersen, E. B. (2002) Renal and cardiac function during alpha1-beta-blockade in congestive heart failure. *Scand. J. Clin. Lab. Invest.* **62**: 97–104

Ishii, Y., Sawada, T., Kubota, K., Fuchinoue, S., Teraoka, S., Shimizu, A. (2005) Injury and progressive loss of peritubular capillaries in the development of chronic allograft nephropathy. *Kidney Int.* **67**: 321–332

Kaijser, M., Johnsson, C., Zezina, L., Backman, U., Dimeny, E., Fellstrom, B. (1997) Elevation of cyclosporin A blood levels during carvedilol treatment in renal transplant patients. *Clin. Transplant.* **11**: 577–581

Kakumoto, M., Sakaeda, T., Takara, K., Nakamura, T., Kita, T., Yagami, T., Kobayashi, H., Okamura, N., Okumura, K. (2003) Effects of carvedilol on MDR1-mediated multidrug resistance: comparison with verapamil. *Cancer Sci.* **94**: 81–86

Katsura, T., Inui, K. (2003) Intestinal absorption of drugs mediated by drug transporters: mechanisms and regulation. *Drug Metab. Pharmacokinet.* **18**: 1–15

Koselj, M., Bren, A., Kandus, A., Kovac, D. (1994) Drug interactions between cyclosporine and rifampicin, erythromycin, and azoles in kidney recipients with opportunistic infections. *Transplant. Proc.* **26**: 2823–2824

Lamba, J. K., Lin, Y. S., Schuetz, E. G., Thummel, K. E. (2002) Genetic contribution to variable human CYP3A-mediated metabolism. *Adv. Drug Deliv. Rev.* **54**: 1271–1294

Lindholm, A. (1991) Factors influencing the pharmacokinetics of cyclosporine in man. *Ther. Drug Monit.* **13**: 465–477

Lown, K. S., Mayo, R. R., Leichtman, A. B., Hsiao, H. L., Turgeon, D. K., Schmiedlin-Ren, P., Brown, M. B., Guo, W., Rossi, S. J., Benet, L. Z., Watkins, P. B. (1997) Role of intestinal P-glycoprotein (mdr1) in interpatient variation in the oral bioavailability of cyclosporine. *Clin. Pharmacol. Ther.* **62**: 248–260

Padi, S. S., Chopra, K. (2002) Salvage of cyclosporine A-induced oxidative stress and renal dysfunction by carvedilol. *Nephron* **92**: 685–692

Park, J., Ha, H., Kim, M. S., Ahn, H. J., Huh, K. H., Kim, Y. S. (2006) Carvedilol inhibits platelet-derived growth factor-induced extracellular matrix synthesis by inhibiting cellular reactive oxygen species and mitogen-activated protein kinase activation. *J. Heart Lung Transplant.* **25**: 683–689

Patel, M. K., Chan, P., Betteridge, L. J., Schachter, M., Sever, P. S. (1995) Inhibition of human vascular smooth muscle cell proliferation by the novel multi-action antihypertensive agent carvedilol. *J. Cardiovasc. Pharmacol.* **25**: 652–657

Ptachcinski, R. J., Venkataramanan, R., Rosenthal, J. T., Burckart, G. J., Taylor, R. J., Hakala, T. R. (1985) Cyclosporine kinetics in renal transplantation. *Clin. Pharmacol. Ther.* **38**: 296–300

Saeki, T., Ueda, K., Tanigawara, Y., Hori, R., Komano, T. (1993) Human P-glycoprotein transports cyclosporin A and FK 506. *J. Biol. Chem.* **268**: 6077–6080

Sambuy, Y., de Angelis, I., Ranaldi, G., Scarino, M. L., Stammati, A., Zucco, F. (2005) The Caco-2 cell line as a model of the intestinal barrier: influence of cell and culture-related factors on Caco-2 cell functional characteristics. *Cell Biol. Toxicol.* **21**: 1–26

Wu, C. Y., Benet, L. Z., Hebert, M. F., Gupta, S. K., Rowland, M., Gomez, D. Y., Wacher, V. J. (1995) Differentiation of absorption and first-pass gut and hepatic metabolism in humans: studies with cyclosporine. *Clin. Pharmacol. Ther.* **58**: 492–497

Zhu, H. J., Wang, J. S., Markowitz, J. S., Donovan, J. L., Gibson, B. B., Gefroh, H. A., Devane, C. L. (2006) Characterization of P-glycoprotein inhibition by major cannabinoids from marijuana. *J. Pharmacol. Exp. Ther.* **317**: 850–857

Ziemann, C., Burkle, A. Kahl, G. F., Hirsch-Ernst, K. I. (1999) Reactive oxygen species participate in mdr1b mRNA and P-glycoprotein overexpression in primary rat hepatocyte cultures. *Carcinogenesis* **20**: 407–414